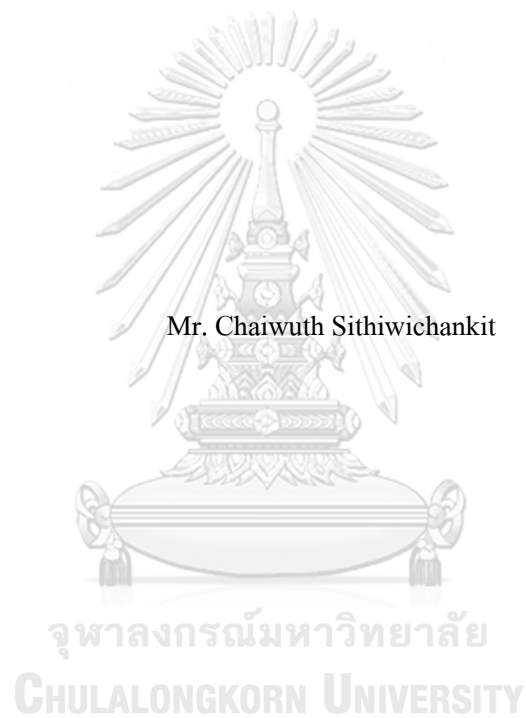


Machine vision integrated three-dimensional printing system



A Thesis Submitted in Partial Fulfillment of the Requirements
for the Degree of Master of Engineering in Mechanical Engineering

Department of Mechanical Engineering

Faculty of Engineering

Chulalongkorn University

Academic Year 2019

Copyright of Chulalongkorn University

ระบบพิมพ์สามมิติแบบบูรณาการแมชชีนวิชั่น



วิทยานิพนธ์นี้เป็นส่วนหนึ่งของการศึกษาตามหลักสูตรปริญญาวิศวกรรมศาสตรมหาบัณฑิต
สาขาวิชาวิศวกรรมเครื่องกล ภาควิชาวิศวกรรมเครื่องกล
คณะวิศวกรรมศาสตร์ จุฬาลงกรณ์มหาวิทยาลัย
ปีการศึกษา 2562
ลิขสิทธิ์ของจุฬาลงกรณ์มหาวิทยาลัย

Thesis Title	Machine vision integrated three-dimensional printing system
By	Mr. Chaiwuth Sithiwichankit
Field of Study	Mechanical Engineering
Thesis Advisor	Associate Professor RATCHATIN CHANCHAROEN, Ph.D.

Accepted by the Faculty of Engineering, Chulalongkorn University in Partial
Fulfillment of the Requirement for the Master of Engineering

..... Dean of the Faculty of Engineering
(Professor SUPOT TEACHAVORASINSKUN, D.Eng.)

THESIS COMMITTEE

..... Chairman
(Professor PAIROD SINGHATANADGID, Ph.D.)

..... Thesis Advisor
(Associate Professor RATCHATIN CHANCHAROEN, Ph.D.)

..... Examiner
(Associate Professor ALONGKORN PIMPIN, D.Eng.)

..... External Examiner
(Lapyote Prasittisopin, Ph.D.)

จุฬาลงกรณ์มหาวิทยาลัย
CHULALONGKORN UNIVERSITY

ชัชวาลิ สิทธิวิจารณ์กิจ : ระบบพิมพ์สามมิติแบบบูรณาการแมชชีนวิชั่น. (Machine vision integrated three-dimensional printing system) อ.ที่ปรึกษาหลัก : รศ. ดร.รัชทิน จันทรเจริญ

การพิมพ์สามมิติเป็นตัวเลือกหนึ่งที่มีการใช้อย่างแพร่หลายสำหรับการผลิตผลิตภัณฑ์ตามความต้องการเชิงรูปทรงของผู้บริโภค โดยทั่วไปตำแหน่งของการพิมพ์สามมิตินิยามอ้างอิงกับระบบพิกัดของเครื่องพิมพ์สามมิติ ดังนั้นการพิมพ์สามมิติจึงไม่สามารถประยุกต์ใช้ได้โดยสะดวกในบางกรณีซึ่งผลิตภัณฑ์ต้องผลิต ณ ตำแหน่งที่อ้างอิงกับวัตถุกายภาพ เช่น การก่อสร้างสถาปัตยกรรม การซ่อมแซมพื้นผิว และการตกแต่งอาหาร เป็นต้น การวิจัยนี้มีจุดประสงค์เพื่อบูรณาการการพิมพ์สามมิติเข้ากับแมชชีนวิชั่นทำให้การพิมพ์สามมิติสามารถประยุกต์ใช้ได้โดยสะดวกในกรณีดังกล่าว โดยระบบพิมพ์สามมิติแบบบูรณาการแมชชีนวิชั่นประกอบด้วย เครื่องพิมพ์สามมิติ กล้องเว็บแคม และเครื่องคอมพิวเตอร์ ในการวิจัยนี้กล้องเว็บแคมถูกติดตั้งเข้ากับหัวพิมพ์ของเครื่องพิมพ์สามมิติและโปรแกรมคอมพิวเตอร์ที่จำเป็นถูกพัฒนาขึ้น จากนั้นทดลองพิมพ์สามมิติบนวัตถุกายภาพเพื่อประเมินความสามารถของระบบพิมพ์สามมิติแบบบูรณาการแมชชีนวิชั่น เนื่องด้วยการพิมพ์สามมิติประสบความสำเร็จด้วยดี ณ ตำแหน่งที่ต้องการ จึงสรุปได้ว่าระบบพิมพ์สามมิติแบบบูรณาการแมชชีนวิชั่นทำให้สามารถประยุกต์ใช้การพิมพ์สามมิติได้โดยสะดวกในกรณีที่กล่าวข้างต้น

จุฬาลงกรณ์มหาวิทยาลัย
CHULALONGKORN UNIVERSITY

สาขาวิชา วิศวกรรมเครื่องกล
ปีการศึกษา 2562

ลายมือชื่อนิติ
ลายมือชื่อ อ.ที่ปรึกษาหลัก

6070421721 : MAJOR MECHANICAL ENGINEERING

KEYWORD: DIGITAL FABRICATION, 3D PRINTING, MACHINE VISION

Chaiwuth Sithiwichankit : Machine vision integrated three-dimensional printing system. Advisor: Assoc. Prof. RATCHATIN CHANCHAROEN, Ph.D.

Three-dimensional printing has been a widespread solution of fabricating geometrical customized products. Any 3D printed product is normally fabricated at a position defined with respect to the coordinate system of the corresponding 3D printer. So, the 3D printing cannot be conveniently implemented in some fabricating applications in which fabricating positions are commonly constrained to some physical references, e.g., architecture construction, surface restoration, food decoration, etc. This research aimed to integrate the 3D printing with machine vision, which is vastly used for guiding robotic systems to operate at desirable positions constrained to physical objects. Hence, the 3D printing can be conveniently and affordably implemented at any position constrained to any physical reference. The proposed machine vision integrated 3D printing system comprises a 3D printer, which is originally constructed in this research, a commercial web camera, and a commercial computer. The web camera was equipped to the printhead of the 3D printer, and necessary computer programs were developed. Then, evaluating products were fabricated on evaluating physical reference, in order to evaluate the machine vision integrated 3D printing system. From the successfully fabricated results of the evaluating products, the machine vision integrated 3D printing system gives promise of conveniently, affordably, and accurately, implementing the 3D printing in the mentioned applications.

Field of Study: Mechanical Engineering

Student's Signature

Academic Year: 2019

Advisor's Signature

ACKNOWLEDGEMENTS

Firstly, I would like to thank Assoc. Prof. Ratchatin Chanchareon, as my thesis adviser, for giving meaningful suggestions on completing this thesis for years. Moreover, he also gave me many opportunities of participating research projects. Throughout these projects, I gained various skills useful for finishing this thesis. Lastly, I would like to express my gratitude to Mr. Suchat Sithiwichankit and Mrs. Aree Sithiwichakit, as respective my father and mother, for their lovely and unconditioned support in several aspects. With their support, I had done this thesis consciously.

Chaiwuth Sithiwichankit



TABLE OF CONTENTS

	Page
ABSTRACT (THAI).....	iii
ABSTRACT (ENGLISH).....	iv
ACKNOWLEDGEMENTS.....	v
TABLE OF CONTENTS.....	vi
LIST OF TABLES.....	ix
LIST OF FIGURES.....	x
CHAPTER 1 INTRODUCTION.....	1
1.1 Motivation.....	1
1.2 Objective.....	2
1.3 Scope.....	2
1.4 Approach.....	2
1.5 Outline.....	3
CHAPTER 2 LITERATURE REVIEW.....	4
2.1 Three-dimensional printing.....	4
2.1.1 Background.....	4
2.1.2 Fabricating any product at any position constrained to any physical reference.....	7
2.2 Machine Vision.....	9
2.2.1 Background.....	9
2.2.2 Guiding robotic systems to desirable operating positions.....	10
2.2.3 Image projection of any digital image.....	11
2.2.4 Estimating the position of any physical point via any two-view image pair.....	13

CHAPTER 3 SYSTEM DESIGN	15
3.1 Three-dimensional printing	15
3.1.1 Acceptable printing organizations of applicable printing techniques	15
3.1.2 Hardware	16
3.1.3 Software	19
3.2 Machine vision	22
3.2.1 Printer-camera calibration.....	22
3.2.2 Hardware	23
3.2.3 Software	23
3.3 System integration.....	27
3.3.1 New expression of Gcode motion commands.....	27
3.3.2 Hardware	28
3.3.3 Software	28
CHAPTER 4 EVALUATION	30
4.1 Printing capability	30
4.1.1 Creating the STL model of the printing-capability evaluating product	30
4.1.2 Generating the Gcode command list of the printing-capability evaluating product	31
4.1.3 Estimating the position of the printing-capability evaluating physical reference.....	32
4.1.4 Fabricating the printing-capability evaluating product	34
4.2 Printing inaccuracy.....	35
4.2.1 Fabricating the printing-inaccuracy evaluating products	36
4.2.2 Estimating the deviated positions of the printing-inaccuracy evaluating products ...	37
CHAPTER 5 CONCLUSION.....	39
5.1 Research conclusion.....	39

5.2 Recommendation.....	40
REFERENCES	41
VITA	46



LIST OF TABLES

	Page
Table 1	Basic characteristics of widespread techniques of the 3D printing6
Table 2	Command types of Gcode frequently used in the 3D printing.21
Table 3	The deviated positions of the printing-inaccuracy evaluating products.38



LIST OF FIGURES

	Page
Figure 1 The unit cost of production due to product quantity of the 3D printing and the typical molding.	5
Figure 2 Sold quantity of 3D printing systems reported by Wohlers Associates, Inc. [3].	5
Figure 3 The process flow of fabricating any product using the 3D printing.	7
Figure 4 An example of implementing the 3D printing for fabricating a product at a position constrained to a physical reference [7].	8
Figure 5 An example of classifying agricultural products using the machine vision [22].	10
Figure 6 The process flow of observing any physical object using the machine vision.	10
Figure 7 The central projection of any single image.	11
Figure 8 The central projection of any two-view image pair.	13
Figure 9 The acceptable printing organization of the LDM printing.	16
Figure 10 The designed and constructed 3D printer.	17
Figure 11 The printing material extruder of the designed and constructed 3D printer.	17
Figure 12 The electrical connection of the designed and constructed 3D printer.	18
Figure 13 The collaboration of the software of the 3D printing.	19
Figure 14 The coordinate systems of the machine vision integrated 3D printing system.	22
Figure 15 The collaboration of the software of the machine vision.	24
Figure 16 The process flow of fabricating any product at any position constrained to any physical reference using the machine vision integrated 3D printing system.	28
Figure 17 The collaboration of the software of the system integration.	29
Figure 18 The design of the printing-capability evaluating product.	30

Figure 19	The printing-capability evaluating product in the printing-description generating program.....	31
Figure 20	The acquired two-view image pair of the printing-capability evaluating physical reference.	32
Figure 21	The corners of the printing-capability evaluating physical reference extracted from the primary image of the acquired two-view image pair of the evaluating physical reference.	33
Figure 22	The corners of the printing-capability evaluating physical reference physical reference tracked in the secondary image of the acquired two-view image pair of the evaluating physical reference.	34
Figure 23	The estimated coordinate system of the printing-capability evaluating physical reference.	34
Figure 24	The fabricated result of the printing-capability evaluating product.	35
Figure 25	The printing-inaccuracy evaluating products in the printing-description generating program.....	36
Figure 26	The fabricated results of the printing-inaccuracy evaluating products.....	37

CHAPTER 1

INTRODUCTION

This chapter introduces the motivation, objective, scope, and approach, of this research. In addition, the outline of this thesis is also informed in this chapter. Accordingly, these topics are separately mentioned in five parts of this chapter.

1.1 Motivation

Since customers accepted paying reasonably higher cost for products achieving their particular requirements, product variety has been a critical issue of business. Because the growth of the product variety raises both opportunity and risk, product customization became a key to success in business competition [1, 2]. Due to the capability of fabricating products of various geometries using any same facility, three-dimensional (3D) printing has been a widespread solution of fabricating geometrically customized products. Furthermore, the 3D printing also enable many fabricating applications, unworthy to be automated with any inflexible automation system, to be automated at affordable cost [3, 4].

In some fabricating applications, any fabricated product is difficult to be manipulated, while geometrical product customization is preferable, e.g., architecture construction, structure restoration, food decoration, etc. In these applications, any product must be fabricated at the corresponding functional position, which is normally constrained to a physical reference [5]. For any 3D printed product, the fabricated position is generally specified with respect to the coordinate system of the corresponding 3D printer [6]. So, the position of any physical reference in these applications must be determined with respect to the coordinate system any 3D printer, in order to enable the 3D printing in these applications. While regular 3D printers cannot observe any physical object, effortful measurement is necessary for determining the position, with respect to the coordinate system of any 3D printer, of any physical reference. Therefore, the 3D printing could not be conveniently implemented in these applications [7].

Recently, few published researches mentioned the idea of integrating a guiding system of laser scanning to a 3D printer, as a solution of conveniently implementing the 3D printing for fabricating any product at any desirable position constrained to any physical reference [5, 8]. The

laser scanning is complicated in implementation, and commonly requires instruments of costly and unwieldy [9]. In order to popularize the 3D printing in the mentioned applications, any guiding system integrated to any 3D printer should be affordable, compact, and simple in implementation. These characteristics match to most of guiding systems of machine vision. For decades, the machine vision has been used for guiding many robotic system to desirable operating positions [10, 11]. Therefore, integrating a guiding system of the machine vision to a 3D printer is an attractive solution of conveniently and affordably implementing the 3D printing for fabricating any product at any position constrained to any physical reference.

1.2 Objective

The objective of this research is proposing machine vision integrated 3D printing system, in which the machine vision is integrated to the 3D printing. Consequently, the 3D printing can be conveniently and affordably implemented for fabricating any product at any position constrained to any physical reference.

1.3 Scope

The scope of this research covers designing and constructing a 3D printer, capable of achieving the research objective, integrating a machine vision system to the designed and constructed 3D printer, and evaluating the machine vision integrated 3D printing system, on fabricating any product at any position constrained to any physical reference.

1.4 Approach

In order to achieve the research objective, the 3D printer, the cartesian motion of which is specifically provided to the printhead, was firstly designed and constructed. Then, the machine vision system was integrated to the 3D printer, by equipping a web camera to the floating end of the 3D printer, and developing necessary computer programs. Finally, evaluated products were fabricated at positions constrained to evaluated physical references using the machine vision integrated 3D printing system.

1.5 Outline

Excluding the introduction, this thesis was organized into four chapters. The result of reviewing on the 3D printing and the machine vision is addressed in Chapter 2. Next, the design of the machine vision integrated 3D printing system is expressed in Chapter 3. Later, the process and result of evaluating the machine vision integrated 3D printing system, on fabricating any product at any position constrained to any physical reference, is mentioned in Chapter 4. Finally, this research is concluded in Chapter 5.



CHAPTER 2

LITERATURE REVIEW

This chapter expresses the result of reviewing on the 3D printing and the machine vision. Therefore, this chapter comprises two main parts, including the 3D printing and the machine vision. The background of the 3D printing, and fabricating any product at any position constrained to any physical reference, are included in the earlier part. In the later part, the background of the machine vision, guiding robotic systems to desirable operating positions, image projection of any digital image, and estimating the position of any physical point via any two-view image pair, are involved.

2.1 Three-dimensional printing

2.1.1 Background

The 3D printing is commonly referred to digital fabrication using additive manufacturing operation [4, 12]. Specifically, the digital fabrication is the process of fabricating any physical product from the corresponding digital information model using fully automated manufacturing, while any manufacturing system of the digital fabrication must be capable of fabricating various product types without any modification on the manufacturing system [13]. In addition, the additive manufacturing operation is the processing operation of shaping any product by adding and solidifying material without any mold [14, 15]. As a flexible manufacturing process, the 3D printing consumes consistent unit cost of production [16]. Thus, the 3D printing is widely used for fabricating geometrically customized products. Moreover, the 3D printing also enable many fabricating applications, products of which are required in small quantity, and unworthy to be fabricated by any inflexible automation system, to be automated at affordable cost [3, 4]. The main strength of the 3D printing is giving consistent unit cost of production due to product quantity. The unit cost of production due to product quantity of the 3D printing is compared with the unit cost of production due to product quantity of typical molding in Figure 1. Meanwhile, the prevalence of the 3D printing can be perceived with the sold quantity of 3D printing systems during 1988 to 2006 reported by Wohlers Associates, Inc., as demonstrated in Figure 2.

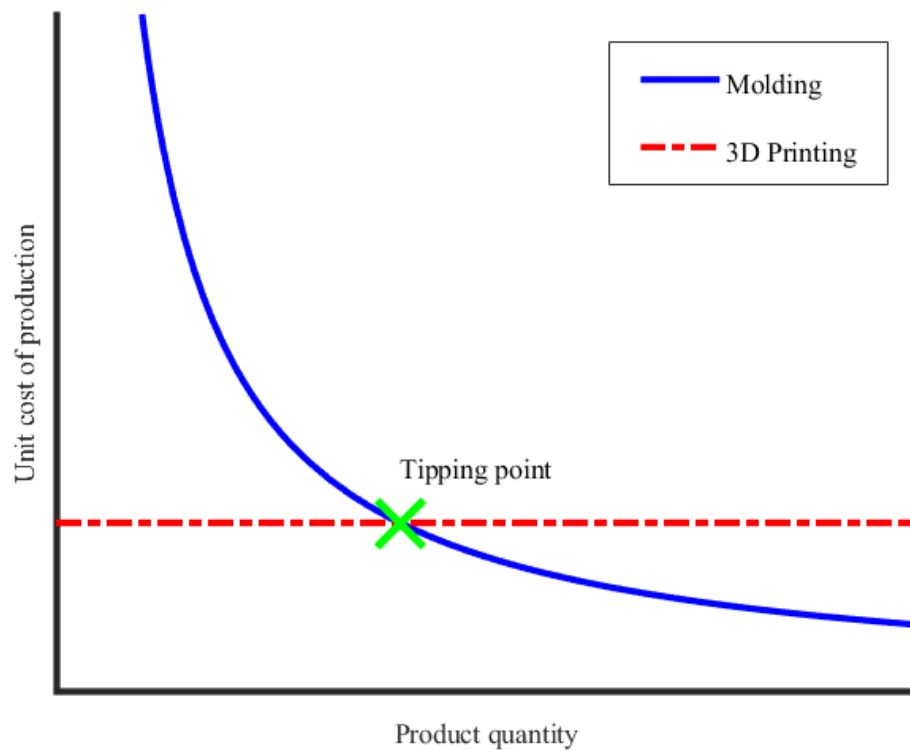


Figure 1 The unit cost of production due to product quantity of the 3D printing and the typical molding.

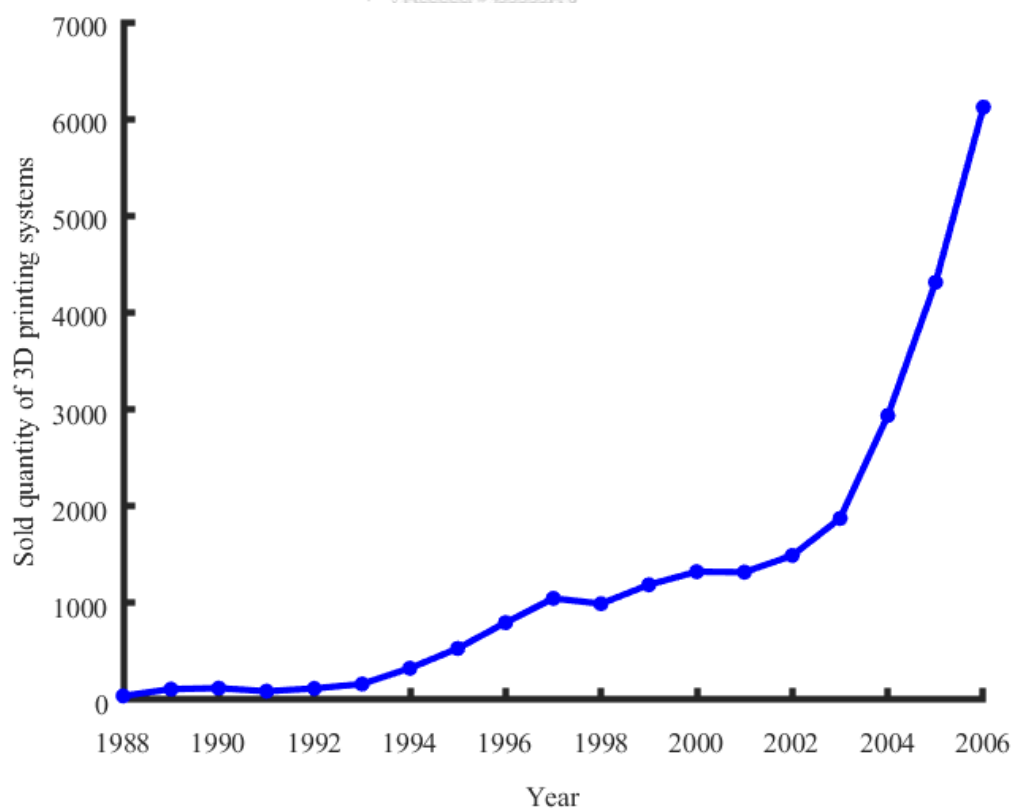


Figure 2 Sold quantity of 3D printing systems reported by Wohlers Associates, Inc. [3].

In order to fabricate any product using the 3D printing, many printing techniques are available for various printing materials and conditions, e.g., fused deposition material (FDM), liquid deposition material (LDM), laminate object manufacturing (LOM), stereolithography (SLA), selective laser sintering (SLS), etc. [15, 17]. Consequently, the 3D printing can be operated at dissimilar conditions with various materials, using different printing techniques. Furthermore, most of printing techniques are layer-by-layer techniques, in which any product is divided into layers, and all layers are created with the same process for any particular printing technique [15]. The mentioned printing techniques are briefly described in Table 1.

Table 1 Basic characteristics of widespread techniques of the 3D printing.

Technique	Available material	Process of each layer
FDM	Polymer filament	Fusing a material filament with heat, extruding the fused material through a small hollow at desirable positions, and cooling the extruded material for the solidification
LDM	Liquid of polymer and ceramic	Extruding material liquid through a small hollow at desirable positions, and solidifying the extruded material with various kinds of mechanism
LOM	Sheet of polymer and metal	Cutting a material sheet into a desirable shape, and joining the cut material with various kinds of mechanism
SLA	Polymer liquid	Pouring material liquid into a container, and exposing the curable frequency laser onto the poured material at desirable positions for solidification
SLS	Powder of polymer and metal	Feeding material powder into a container, and exposing the absorbable frequency laser of on to the fed material at desirable positions for heat joining

In order to fabricate any product using the 3D printing, the starting step is designing and creating the corresponding digital information model of the product. Next, the printing configuration of the product is customized, and related constraints of the corresponding 3D printer are identified. Then, the printing description of the product is generated. Later, the generated printing description is transferred to the controller of the corresponding 3D printer. Finally, the corresponding 3D printer fabricates the product until the fabrication is finished [6]. The process flow of fabricating any product using the 3D printing is illustrated in Figure 3.

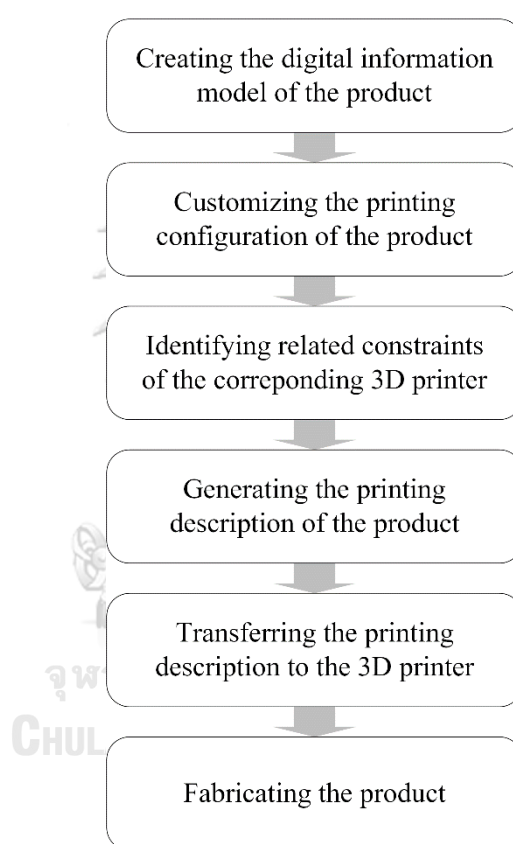


Figure 3 The process flow of fabricating any product using the 3D printing.

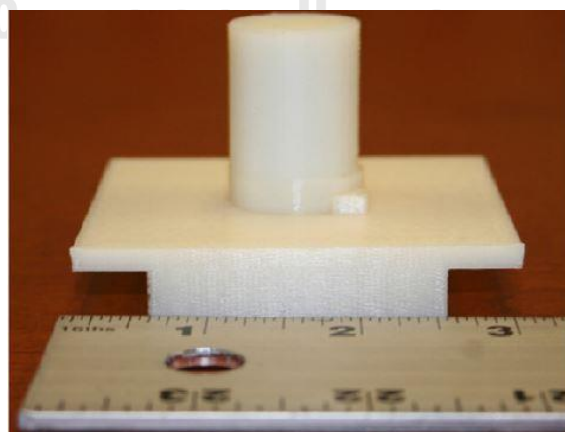
2.1.2 Fabricating any product at any position constrained to any physical reference

In some fabricating applications, manipulation on any fabricated product consumes massive effort and endurance. So, any product in these must be fabricated at the corresponding functional position, which is commonly constrained to a physical reference. Moreover, any product in these applications is also normally fabricated at small quantity. Hence, the geometrical product customization is preferable in these applications. Examples of these applications are

architecture construction, structure restoration, food decoration, etc. Recently, the 3D printing became an interesting solution of the geometrical product customization in these applications [5]. Generally, the fabricated position of any 3D printed product is specified with respect to the coordinate system of the corresponding 3D printer [6]. In order to fabricate any product in these applications at any position using the 3D printing, the position of any physical reference in these applications must be determined with respect to the coordinate system of any 3D printer. Therefore, the fabricated position of any product in these applications can be determined with respect to the coordinate system of the corresponding 3D printer. However, regular 3D printers are incapable of observing any physical object, while hardworking measurement is necessary for determining the position, with respect to the coordinate system of any 3D printer, of any physical object. Consequently, the 3D printing was unable to be conveniently implemented in these applications [7]. An example of implementing the 3D printing for fabricating a position constrained a physical reference is demonstrated in Figure 4.



(a) The referencing base



(b) The printing result

Figure 4 An example of implementing the 3D printing for fabricating a product at a position constrained to a physical reference [7].

Over last few years, the idea of integrating the laser scanning to the 3D printing for fabricating any product at any desirable position constrained to any physical reference using the 3D printing appeared in few published researches. [5, 8]. However, most of laser scanners are normally expensive and unwieldy, while the laser scanning is sophisticated in implementation [9]. Contrastively, any guiding system integrated to any 3D printer should be affordable, compact, and effortless in implementation, in order to make the 3D printing widespread in the mentioned applications. These characteristics match to most of guiding systems of machine vision since guiding systems of the machine vision are commonly inexpensive and compact, and the machine vision can be easily and flexibly implemented [10]. Furthermore, guiding the systems of assembly and welding to accurately operate at desirable positions using the machine vision, was previously introduced in published researches [9, 18]. Consequently, integrating a machine vision system to a 3D printer is an interesting solution of conveniently affordably implementing the 3D printing for fabricating any product at any desirable position constrained to any physical reference.

2.2 Machine Vision

2.2.1 Background

The machine vision is vastly referred to the process of giving physical perception to any automation system via some digital images. In addition, digital images employed in the machine vision can be captured using various camera types. Basically, the physical perception provided by the machine vision is applicable for three main functions, including classifying, locating, and inspecting, physical objects [10]. These three main functions of applicable of the machine vision cover several tasks, in many applications of various industries, so the machine vision has been widely applied in numerous applications, e.g., robotic-system guidance, vehicle-driving assistance, human-activity recognition, etc. [18-20]. An example of classifying agricultural products using the machine vision is demonstrated in Figure 5.

In order to observe any physical object using the machine vision, the beginning step is acquiring some digital images of the observing physical object. Later, the acquired digital images are processed into any preferable format. Then, image regions containing the observing physical object are segmented from the processed images. Next, informative features of the observing physical object are extracted from the segmented image regions. Finally, the extracted

informative features are interpreted, for achieving the observing purpose [21]. The process flow of observing any physical object using the machine vision, is illustrated in Figure 6.



Figure 5 An example of classifying agricultural products using the machine vision [22].

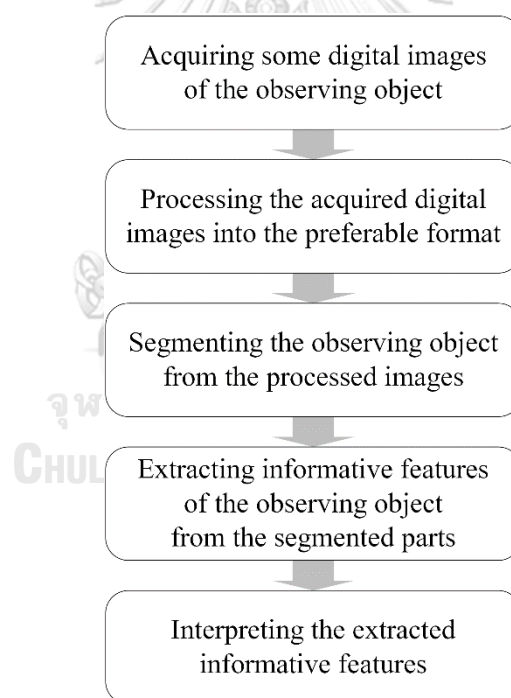


Figure 6 The process flow of observing any physical object using the machine vision.

2.2.2 Guiding robotic systems to desirable operating positions

According to continuous and impactful development of robotics, many manufacturing operations are presently expected to be accurately completed at desirable positions using robotic systems, e.g., assembly, welding, etc. In order to accurately achieve these manufacturing

operations at desirable positions using robotic systems, the robotic systems must be positionally guided [9, 18]. Since the machine vision is capable of three-dimensionally locates various physical objects, manufacturing operations can be accurately completed at desirable positions using robotic systems guided by the machine vision [10]. Compared with competitive guiding processes, e.g., laser scanning, magnetic resonating, ultrasound echoing, etc., the machine vision is simpler in implementation. In addition, necessary instruments for the machine vision are relatively low-cost and compact [9, 23, 24]. The machine vision consequently has been a widely used solution of guiding robotic systems to desirable operating positions for decades [10, 11].

2.2.3 Image projection of any digital image

Basically, image projection is referred to the process of acquiring image by projecting light onto some corresponding sensing elements. The most usual geometrical model used for describing the image projection is called central projection. Let $\{C\}$ be the cartesian coordinate system of any camera, \hat{I} be the image plane of the camera, $\{I\}$ be the image coordinate system of the camera, f be the focal length of the camera, and x_p be the center of \hat{I} . In the central projection, the light from any point source X is projected through \hat{I} to the origin of $\{C\}$, which is usually called center of projection. The point at which the light projected from X pass through \hat{I} is the corresponding image point x of X . Ideally, x_p , usually called principal point, is at the distance of f from the origin of $\{C\}$ along the Z-axis of $\{C\}$. Meanwhile, $\{I\}$ is parallel to the XY-plane of $\{C\}$ [25]. The central projection of any single image is illustrated in Figure 7.

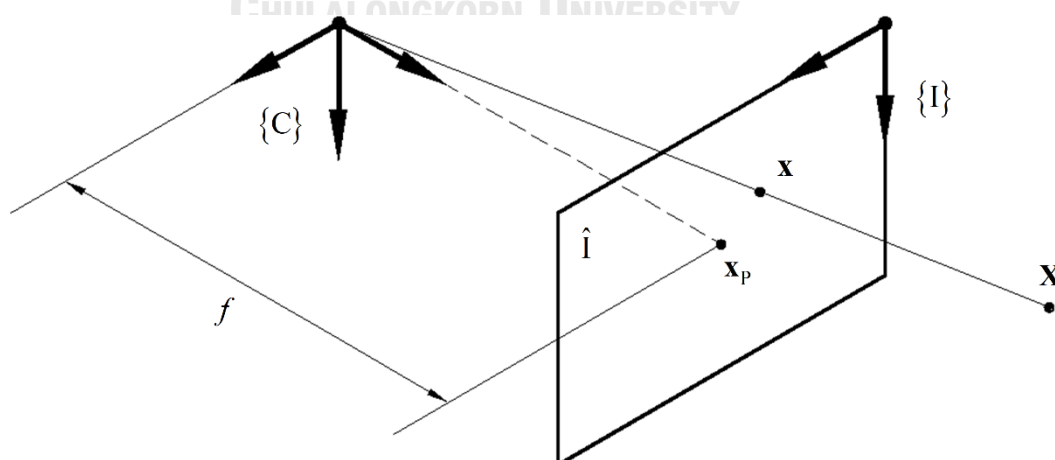


Figure 7 The central projection of any single image.

In expression, \mathbf{X} is characterized by the corresponding position, with respect to $\{C\}$, as $\mathbf{X} = [X \ Y \ Z \ 1]^T$, while \mathbf{x} is characterized by the corresponding position, with respect to $\{I\}$, as $\mathbf{x} = [x \ y \ 1]^T$. Furthermore, \mathbf{x}_p is expressed with the corresponding position, with respect to $\{I\}$, as $\mathbf{x}_p = [x_p \ y_p \ 1]^T$. Mathematically, the correlation between \mathbf{X} and \mathbf{x} is able to be written as follows,

$$w\mathbf{x} = \mathbf{K}\mathbf{X} = \begin{bmatrix} f & s & x_p & 0 \\ 0 & f & y_p & 0 \\ 0 & 0 & 1 & 0 \end{bmatrix} \mathbf{X}. \quad (1)$$

The matrix \mathbf{K} , usually called camera matrix, is consistent for any camera, and s is known as skew factor. Furthermore, w is an arbitrary scale factor. Normally, $\{I\}$ is defined in pixel unit, instead of any physical unit. Let \mathbf{u} be the corresponding position in the pixel unit of \mathbf{x} . Meanwhile, \mathbf{u} is expressed with the corresponding position, with respect to $\{I\}$, as $\mathbf{u} = [u \ v \ 1]^T$. The mathematical correlation between \mathbf{u} and \mathbf{x} can be written as follows,

$$\mathbf{u} = \begin{bmatrix} d_u & 0 & 0 \\ 0 & d_v & 0 \\ 0 & 0 & 1 \end{bmatrix} \mathbf{x}. \quad (2)$$

The variables of d_u and d_v , which respectively represent the ratios of u to x , and v to y , are also invariant for any camera [25].

Practically, the image projection may be distorted by camera lenses. The distortion caused by of camera lenses is commonly called lens distortion. The lens distortion can be categorized into two types, including radial distortion and tangential distortion. Let $\partial\mathbf{x}(\mathbf{x})_{\text{radial}}$ and $\partial\mathbf{x}(\mathbf{x})_{\text{tangential}}$ be respective the radial distortion and the tangential distortion at \mathbf{x} . Meanwhile, $\partial\mathbf{x}(\mathbf{x})_{\text{radial}}$ is expressed as $\partial\mathbf{x}(\mathbf{x})_{\text{radial}} = [\partial x(\mathbf{x})_{\text{radial}} \ \partial y(\mathbf{x})_{\text{radial}} \ 0]^T$, and $\partial\mathbf{x}(\mathbf{x})_{\text{tangential}}$ is expressed as $\partial\mathbf{x}(\mathbf{x})_{\text{tangential}} = [\partial x(\mathbf{x})_{\text{tangential}} \ \partial y(\mathbf{x})_{\text{tangential}} \ 0]^T$. Mathematically, $\partial\mathbf{x}(\mathbf{x})_{\text{radial}}$ and $\partial\mathbf{x}(\mathbf{x})_{\text{tangential}}$ can be sequentially resolved as follows,

$$\partial\mathbf{x}(\mathbf{x})_{\text{radial}} = \left(1 + \sum_{i=1}^n k_i r^{2i} \right) \begin{bmatrix} x \\ y \\ 0 \end{bmatrix} \quad (3)$$

, and

$$\partial\mathbf{x}(\mathbf{x})_{\text{tangential}} = \begin{bmatrix} 2(x-x_p)(y-y_p) & r^2 + 2(x-x_p)^2 & 0 \\ r^2 + 2(y-y_p)^2 & 2(x-x_p)(y-y_p) & 0 \end{bmatrix} \begin{bmatrix} p_x \\ p_y \\ 0 \end{bmatrix}. \quad (4)$$

The variable r is defined as $r = \sqrt{(x - x_p)^2 + (y - y_p)^2}$. Meanwhile, k_i is the radial-distortion coefficient of i^{th} order, and n is the largest estimation order of the radial distortion. Furthermore, p_x and p_y are the tangential-distortion coefficients. In order to resolve (3) and (4), nonlinear optimization is necessary. After $\partial \mathbf{x}(\mathbf{x})_{\text{radial}}$ and $\partial \mathbf{x}(\mathbf{x})_{\text{tangential}}$ are determined, the lens distortion at \mathbf{x} can be corrected as follows,

$$\mathbf{x}_{\text{Corrected}} = \mathbf{x} + \partial \mathbf{x}(\mathbf{x})_{\text{radial}} + \partial \mathbf{x}(\mathbf{x})_{\text{tangential}} \quad (5)$$

, where $\mathbf{x}_{\text{Corrected}}$ represents the corrected point of \mathbf{x} [26].

2.2.4 Estimating the position of any physical point via any two-view image pair

In the image projection, any 3D point \mathbf{X} is transformed into the corresponding two-dimensional (2D) point \mathbf{x} . Therefore, \mathbf{X} is obviously unable to be determined from any single image. In order to uniquely determine \mathbf{X} , multiple-view images of \mathbf{X} are required. Minimally, \mathbf{X} can be uniquely determined from any two-view image pair of \mathbf{X} [27]. The central projection of any two-view image pair is illustrated in Figure 8.

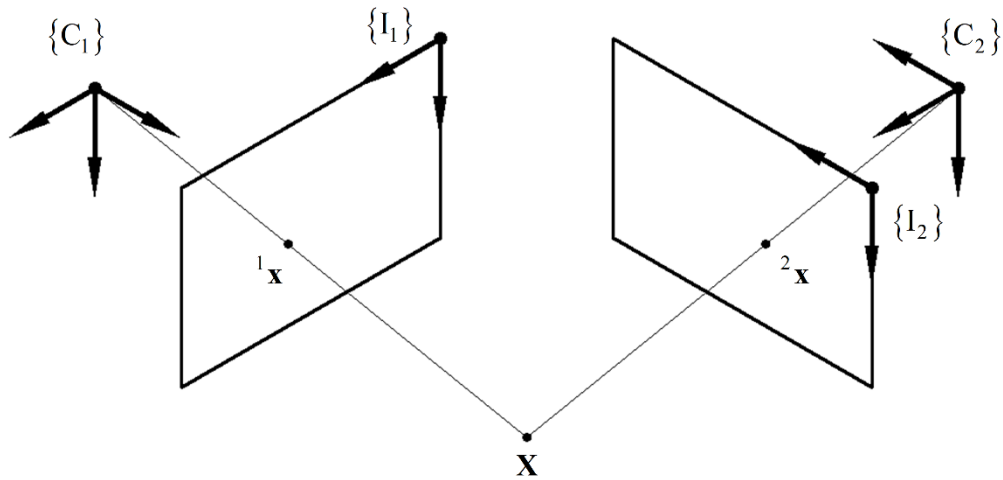


Figure 8 The central projection of any two-view image pair.

Let ${}^i \mathbf{X} = [{}^i X \quad {}^i Y \quad {}^i Z \quad 1]^T$ be the position, with respect to $\{C_i\}$, of \mathbf{X} , ${}^i \mathbf{x} = [{}^i x \quad {}^i y \quad 1]$ be the position, with respect to $\{I_i\}$, of \mathbf{x} , and ${}^i w$ be any arbitrary scale factor of ${}^i \mathbf{x}$. In order to uniquely determine ${}^1 \mathbf{X}$ or ${}^2 \mathbf{X}$ from any two-view image pair of \mathbf{X} , ${}^1 \mathbf{x}$ and ${}^2 \mathbf{x}$ must be accurately extracted from the two-view images [28]. If the two-view images are acquired with the same camera, ${}^1 w {}^1 \mathbf{x} = \mathbf{K} {}^1 \mathbf{X}$ and ${}^2 w {}^2 \mathbf{x} = \mathbf{K}_1 {}^2 \mathbf{H} {}^1 \mathbf{X}$ can be obtained by extending (1), where the

matrix ${}^2_1\mathbf{H}$ is the homogeneous transformation matrix from $\{C_1\}$ to $\{C_2\}$. Thus, these obtained equations can be transformed as follows,

$$\mathbf{K}^1\mathbf{X} - {}^1w^1\mathbf{x} = \mathbf{0} \quad (6)$$

, and

$$\mathbf{K}^2_1\mathbf{H}^1\mathbf{X} - {}^2w^2\mathbf{x} = \mathbf{0}. \quad (7)$$

By combining (6) and (7), six independent scalar equations are acquired. Clearly, ${}^1\mathbf{X}$, 1w , and 2w , which totally consist of five scalar variables, are resolvable from the acquired scalar equations. The acquired scalar equations can be transformed into a matrix equation as follows,

$$\begin{bmatrix} f & s & x_p & 0 \\ 0 & f & y_p & 0 \\ 0 & 0 & 1 & 0 \\ fh_{11} + sh_{21} + x_ph_{31} & fh_{12} + sh_{22} + x_ph_{32} & fh_{13} + sh_{23} + x_ph_{33} & fh_{14} + sh_{24} + x_ph_{34} \\ fh_{21} + y_ph_{31} & fh_{22} + y_ph_{32} & fh_{23} + y_ph_{33} & fh_{24} + y_ph_{34} \\ h_{31} & h_{32} & h_{33} & h_{34} \end{bmatrix} {}^1\mathbf{X} = \begin{bmatrix} {}^1w^1x \\ {}^1w^1y \\ {}^1w \\ {}^2w^2x \\ {}^2w^2y \\ {}^2w \end{bmatrix} \quad (8)$$

, where h_{ab} is the element of row a and column b of ${}^2_1\mathbf{H}$. Geometrically, 1Z is greater than f . Consequently, ${}^1\mathbf{X}$ can be uniquely resolved as the linear solution of (8) [27].

CHAPTER 3

SYSTEM DESIGN

The design of the machine vision integrated 3D printing system is expressed in this chapter. In composition, the design was classified into three main parts, including the 3D printing, the machine vision, and the system integration. In the first part, acceptable printing organizations of applicable printing techniques, and the hardware and software of the 3D printing, are involved. Meanwhile, the second part includes printer-camera calibration, and the hardware and software of the machine vision. Lastly, the third part mentions new expression of Gcode motion commands, and the hardware and software of the system integration.

3.1 Three-dimensional printing

3.1.1 Acceptable printing organizations of applicable printing techniques

In this research, the 3D printing is originally expected to be implemented for fabricating any product at the corresponding functional position, which is vastly constrained to a physical reference. The corresponding functional position of any physical reference may be laid on any sensitive platform, which is able to be easily destroyed by some handling. Therefore, any handling on printing platform fundamentally must be unnecessary for the 3D printing in this research. Among many available printing techniques, some printing techniques fabricate any product in some printing material containers, e.g., SLA, SLS, etc. Somehow, printing material containers, as the printing platform, need to be handled in these printing techniques. Hence, these printing techniques is inapplicable in this research. Alternatively, some other printing techniques are capable of fabricating any product without any handling on the printing platform, e.g., FDM, LDM, LOM, etc. Additionally, only some printing organizations of these printing techniques, which are able to three-dimensionally deliver printing material without any handling on the printing platform, are acceptable in this research. The acceptable printing organization of the LDM printing is illustrated in Figure 9.

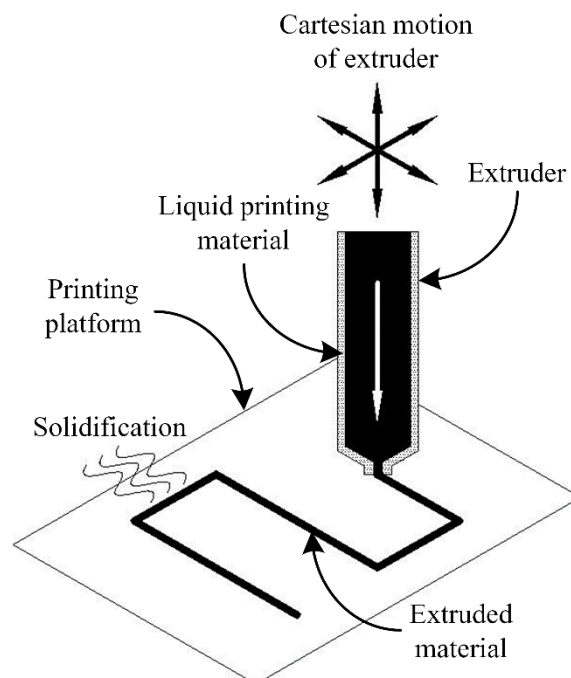


Figure 9 The acceptable printing organization of the LDM printing.

3.1.2 Hardware

Excluding a computer, the hardware of the 3D printing, is entirely included in the 3D printer originally designed and constructed in this research. Basically, the 3D printer is an LDM printer, the 3D motion of which is provided at the printhead of the 3D printer. Meanwhile, the printing platform is not included in the 3D printer. In addition, the hardware of the 3D printer comprises three components, including a printing material extruder, a three-axis manipulator, and a 3D-printer controller. The designed and constructed 3D printer is demonstrated in Figure 10.

The printing material extruder can be classified as a ram extruder [29], while the role of the printing material extruder is delivering the printing material. So, the printing material can be extruded and retracted at preferable amount. For handling the printing material, a 10-ml plastic medical syringe [30] is instantaneously used. If any equipped syringe is run out of the printing material, the syringe is disposed and replaced, by another fully filled syringe. In order to actuate and transmit extrusion and retraction of the printing material, a stepper motor [31] and a ball-screw drive [32] are respectively used. The barrel and the plunger of the equipped syringe are respectively mounted to the fixed side and the floating side of the ball-screw drive. In order to vary venting diameter of the printing material, plastic dispenser needles of various sizes are used. The printing material extruder of the designed and constructed 3D printer is shown in Figure 11.

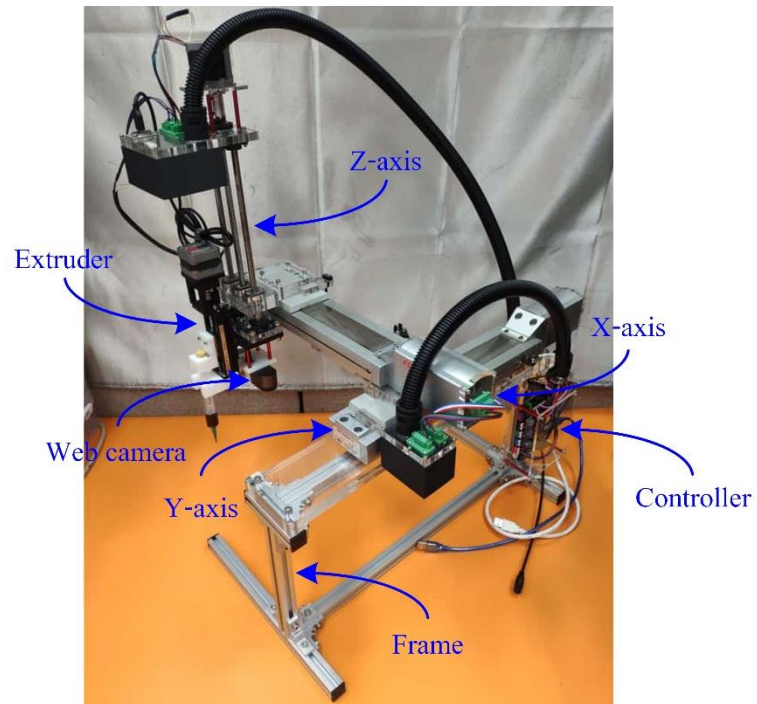


Figure 10 The designed and constructed 3D printer.

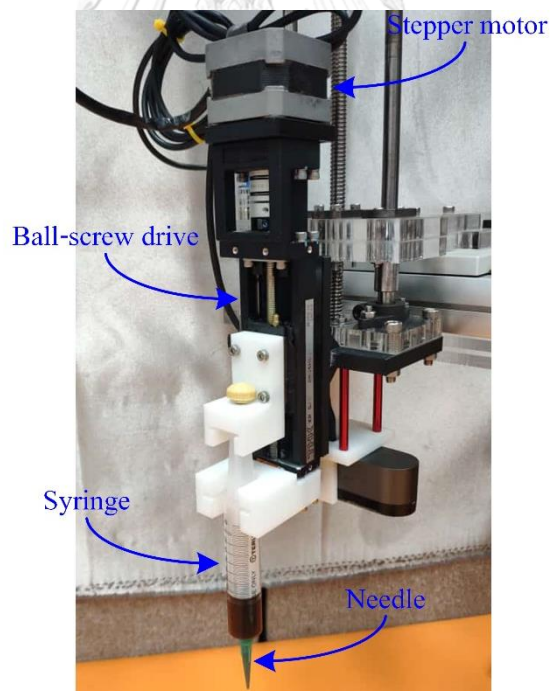


Figure 11 The printing material extruder of the designed and constructed 3D printer.

The three-axes manipulator can be classified as a three-axes cartesian manipulator [33], while the responsibility of the three-axis manipulator is three-dimensionally moving the printing material extruder, which was mounted to the floating end of the three-axes manipulator. In order

to actuate the three-axis manipulator, a stepper motor and a ball-screw drive are employed in each axis, while the axes of any three-axis cartesian manipulator are usually called as X-axis, Y-axis, and Z-axis. In arrangement, the fixed side of the Y-axis ball-screw drive was mounted to an aluminium extrusion frame, the floating side of the Y-axis ball-screw drive was mounted to the fixed side of the X-axis ball-screw drive, and the floating side of the X-axis ball-screw drive was mounted to the floating side of the Z-axis ball-screw drive. For perceiving the absolute position of each stepper motor of the three-axis manipulator, two optical proximity sensors [31] were fixed to the X-axis ball-screw drive and the Y-axis ball-screw drive, and a magnetical proximity sensor [31] was fixed to the Z-axis ball-screw drive.

The 3D-printer controller can be classified as a microcontroller board [31], specifically designed to be an FDM printer controller. Meanwhile, the charge of the 3D-printer controller is providing executional signals to the stepper motors of the printing material extruder and the three-axis manipulator, and responding signals from the proximity sensors of the three-axis manipulator. Meanwhile, the 3D-printer controller is perfectly compatible with stepper motors and proximity sensors. In order to cooperate each stepper motor with the 3D-printer controller, a stepper motor driver [31] is employed. For power supply, an electrical AC to DC adapter is used. The electrical connection of the designed and constructed 3D printer is illustrated in Figure 12.

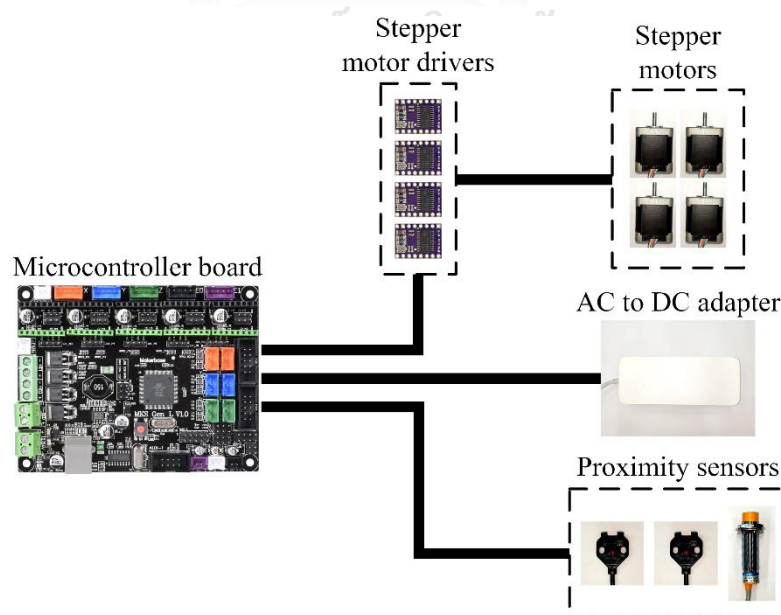


Figure 12 The electrical connection of the designed and constructed 3D printer.

3.1.3 Software

The software of the 3D printing comprises three computer programs, including a digital-model generating program, a printing-description generating program, a printing-description transferring program, and an 3D-printer operating program. The 3D-printer operating program is run on the 3D-printer controller, while the other programs are processed on the computer. The collaboration of the software of the 3D printing is illustrated in Figure 13.

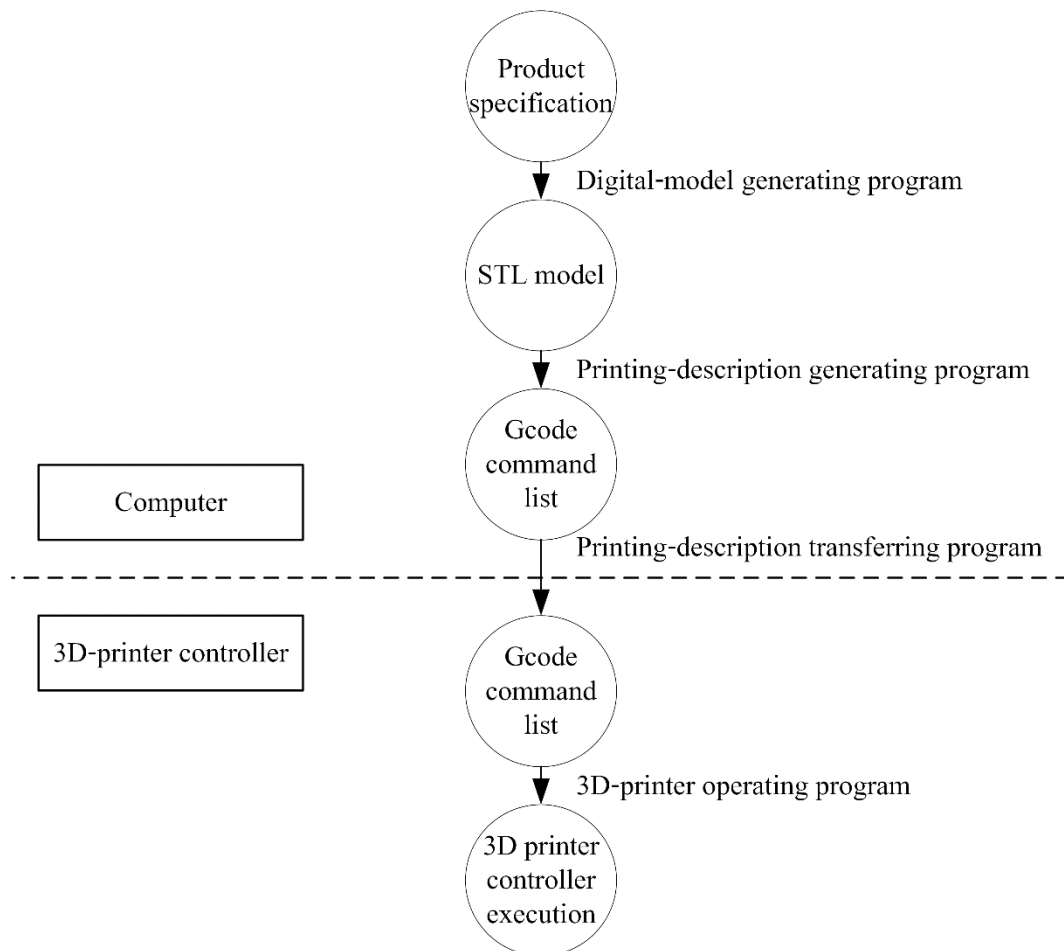


Figure 13 The collaboration of the software of the 3D printing.

The digital-model generating program is primarily accountable of generating the corresponding digital model of any product. In this research, a commercial computer-aided design (CAD) program is used as the digital-model generating program. In the CAD program, the digital model of any product is manually designed, following the specification of the product, and then generated as a stereolithography (STL) model [34].

The printing-description generating program is mainly responsible of generating the printing description of any product, following the STL model of the product. In this research, an open-source program, specifically developed for generating printing descriptions following any STL model, is used as the printing-description generating program. Before the printing description of any product is generated, the printing configuration of the product must be specifically customized, and related constraints of the 3D printer must be accurately identified, in the printing-description generating program. Specifically, any printing description in this case is generated as a command list of Gcode [35]. Command types of Gcode frequently used in the 3D printing are briefly summarized in Table 2.

The printing-description transferring program is principally accountable of transferring Gcode commands from the computer to the 3D-printer controller. In this research, the printing-description transferring program was originally developed. Via serial communication [31], the printing-description transferring program sends Gcode commands to the 3D-printer operating program, synchronously with working of the 3D printer, and also receives and displays printing information returned from the 3D-printer operating program.

The 3D-printer operating program is responsible of managing execution of the 3D-printer controller. In this research, an open-source program, particularly developed to be an FDM printer operating program, is used as the 3D-printer operating program. Since the 3D-printer controller and the 3D-printer operating program are perfectly compatible, the 3D-printer operating program was directly embedded into the 3D-printer controller, via the serial communication. After any Gcode command is acquired into the 3D-printer operating program, via the serial communication, the 3D-printer controller executes the corresponding execution of the Gcode command.

Table 2 Command types of Gcode frequently used in the 3D printing.

Command type	Example	Description
G1	G1 X100 Y150 Z10 E0.5 F3000	Moving the corresponding 3D printer from the current position to the expressed target position at the specified speed, with linear trajectory planning
G4	G4 P3000	Pausing the operation of the corresponding 3D printer for the specified period of time
G20	G20	Setting the positioning unit of the corresponding 3D printer to inch
G21	G21	Setting the positioning unit of the corresponding 3D printer to millimeter
G28	G28 X Y	Moving the corresponding 3D printer from the current position to the position at which the proximity sensors operate
G90	G90	Setting the positioning definition of the manipulator axes of the corresponding 3D printer to be absolute
G91	G91	Setting the positioning definition of the manipulator axes of the corresponding 3D printer to be relative
G92	G92 X0 Y0 Z0 E0	Setting the current position of the corresponding 3D printer to be defined as the specified position
M82	M82	Setting the positioning definition of the extruder axis of the corresponding 3D printer to be absolute
M83	M83	Setting the positioning definition of the extruder axis of the corresponding 3D printer to be relative
M84	M84	Disabling idle hold of all the stepper motors of the corresponding 3D printer
M114	M114	Getting the current position of the corresponding 3D printer

3.2 Machine vision

3.2.1 Printer-camera calibration

Fundamentally, several constant parameters must be calibrated in order to estimate the position of any physical object via any two-view image pair. By considering (8), \mathbf{K} in (1), d_u and d_v in (2), k_i in (3), p_x and p_y in (4), and ${}^2_1\mathbf{H}$ in (7), are the parameters necessary to be calibrated. In this research, \mathbf{K} , d_u , d_v , and ${}^2_1\mathbf{H}$, were determined following the algorithm proposed by Z. Zhang [36], while k_i , p_x , and p_y , were resolved following the procedures presented by J. Heikkila and O. Silven [26].

In order to guide the 3D printer to any position constrained to any physical reference, the correlation between the web-camera coordinate system, denoted by $\{C\}$, and the 3D-printer coordinate system, denoted by $\{P\}$, also need to be calibrated. Thus, the homogeneous transformation matrix from $\{C\}$ to $\{P\}$, denoted with ${}^P_C\mathbf{H}$, was calibrated in this research. Because the web camera was equipped to the printhead of the 3D printer, ${}^P_C\mathbf{H}$ can be split as ${}^P_C\mathbf{H} = {}^P_T\mathbf{H} {}^T_C\mathbf{H}$, where ${}^P_T\mathbf{H}$ and ${}^T_C\mathbf{H}$ sequentially represent the homogeneous transformation matrix from the imaginary coordinate system attached at the printhead tip, denoted by $\{T\}$, to $\{P\}$, and the homogeneous transformation matrix from $\{C\}$ to $\{T\}$. The coordinate systems of the machine vision integrated 3D printing system are demonstrated in Figure 14.

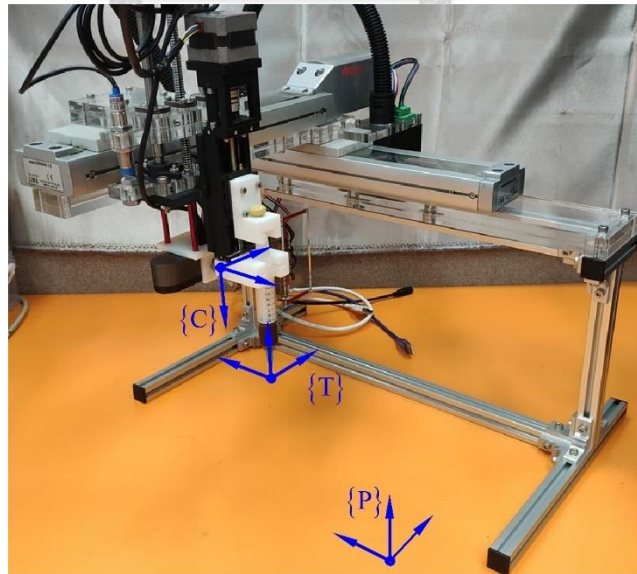


Figure 14 The coordinate systems of the machine vision integrated 3D printing system.

Let ${}^C\mathbf{X}$ be the position, with respect to $\{C\}$, of \mathbf{X} , and ${}^P\mathbf{X}$ be the position, with respect to $\{P\}$, of \mathbf{X} . The mathematical correlation between ${}^C\mathbf{X}$ and ${}^P\mathbf{X}$ can be written as follows,

$${}^T_C\mathbf{H}{}^C\mathbf{X} - {}^T_P\mathbf{H}{}^P\mathbf{X} = \mathbf{0}. \quad (9)$$

Specifically, $\{T\}$ was defined with the same orientation as $\{P\}$. Hence, ${}^T_P\mathbf{H}$ is pure translation, and can be acquired from the 3D-printer controller. For resolving ${}^T_C\mathbf{H}$, the nonlinear least-square optimization proposed by T. F. Coleman and Y. Li [37, 38] was applied on the left side of (9), while ${}^C\mathbf{X}$ and ${}^P\mathbf{X}$ in (9) were turned into the multiple-column matrices of calibration points. Additionally, ${}^T_C\mathbf{H}$ was predefined with Z-Y-X Euler angles [33] and a translation vector as follows,

$${}^T_C\mathbf{H} = \begin{bmatrix} c\theta_1 c\theta_2 & (c\theta_1 s\theta_2 s\theta_3) - (s\theta_1 c\theta_3) & (s\theta_1 s\theta_3) + (c\theta_1 s\theta_2 c\theta_3) & t_x \\ s\theta_1 c\theta_2 & (c\theta_1 c\theta_3) + (s\theta_1 s\theta_2 s\theta_3) & (s\theta_1 s\theta_2 c\theta_3) - (c\theta_1 s\theta_3) & t_y \\ -s\theta_2 & c\theta_2 s\theta_3 & c\theta_2 c\theta_3 & t_z \\ 0 & 0 & 0 & 1 \end{bmatrix}. \quad (10)$$

3.2.2 Hardware

The hardware of the machine vision consists of three parts, including the web camera, the 3D printer, and the computer. In this research, the web camera is a commercial web camera, capable of capturing images at full high definition (FHD) [39] resolution. As shown in Figure 10, the web camera was equipped to the printhead of the 3D printer. The web camera is accountable of acquiring images of any physical reference, while the 3D printer is responsible of moving the web camera. In addition, the charge of the computer is processing and analysing on acquired images, and communicating with the 3D-printer controller.

3.2.3 Software

The software of the machine vision comprises three computer programs, including an image-acquisition program, a feature-extraction program, and a pose-estimation program. Instantaneously, these programs are sequentially run on the computer, for estimating the position, with respect to the 3D-printer coordinate system, of any physical reference. Additionally, these programs were developed in this research. The collaboration of the software of the machine vision is illustrated in Figure 15.

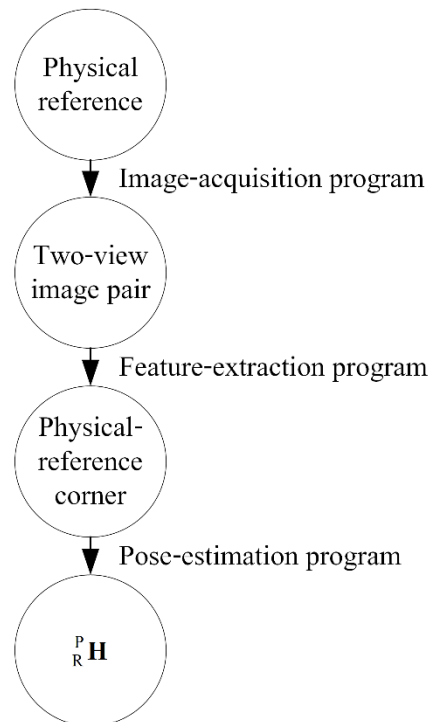


Figure 15 The collaboration of the software of the machine vision.

The image-acquisition program is accountable of acquiring any two-view image pair of any physical reference. Before the image-acquisition program is started, the computer must be connected to the 3D printer and the web camera, and the position of capturing the primary image of any two-view image pair need to be specified. Initially, some Gcode commands are sent to the 3D-printer operating program, in order to move the web camera to the specified position of capturing the primary image of the two-view image pair, after the image-acquisition program is begun. Then, the primary image of the two-view image pair is captured by the web camera, and acquired into the computer, via the serial communication. Next, some Gcode commands are sent to the 3D-printer operating program, in order to move the web camera to the position of capturing the secondary image of the two-view image pair. In addition, the position of capturing the secondary image of the two-view image pair must be predefined relative to the specified position of capturing the primary image of the two-view image pair. In this research, the relative position of where the secondary image of the two-view image pair is captured to where the primary image of the two-view image pair is captured was particularly predefined as 30 mm along the negative direction of the Y-axis of the 3D-printer coordinate system. Finally, the secondary image is captured by the web camera, and acquired into the computer, via the serial communication.

The feature-extraction program is responsible of extracting characteristic features of any physical reference, from any two-view image pair of the physical reference acquired using the image-acquisition program. In this research, the extractable features are only the corners of any rectangular-plate physical reference. Before the feature-extraction program is started, any point in the region of any considering physical reference must be marked in the primary image of any two-view image pair of the physical reference, and any 8-bit RGB color threshold need to be defined. Initially, color thresholding [40] is applied, with the defined 8-bit RGB color threshold, to the primary image of the two-view image pair, in order to segment the image region of the physical reference, after the feature-extraction program is begun. Thus, the resulting binary image, in which the foreground is white, and the background is black, is obtained. Next, the white region of the physical reference in the obtained binary image is programmatically recognized, using blob detection [41] together with the position of the marked point. Later, the corners of the physical-reference region are extracted from the obtained binary image, following the algorithm proposed by J. Shi and C. Tomasi [42], while the corresponding region of interest is given by the blob detection. In this step, Gaussian filtering [43] may be applied to the obtained binary image, in order to minimize error results of the corner extraction, before the corner extraction is commenced. If the corners of the physical reference are rounded, the corner extraction is likely to provide unfilterable error results, around each corner of the physical-reference region. Hence, all extracted results given by the corner extraction are categorized into four groups, using k-means clustering [44]. Accordingly, the average point of each clustered group is defined as a corner of the physical reference in the primary image of the two-view image pair. Finally, the corners of the physical reference in the secondary image of the two-view image pair are tracked, following Kanade–Lucas–Tomasi (KLT) algorithm [45, 46]. Specifically, the KLT algorithm is processed following pyramidal implementation [47] in this research.

The pose-estimation program is in charge of estimating the position, with respect to the 3D-printer coordinate system denoted by $\{P\}$, of any physical reference, from the corners of the physical reference extracted using the feature-extraction program. In this research, only the position of any rectangular-plate physical reference is able to be estimated. Firstly, the effect of the lens distortion is corrected, following (3) to (5). Next, the position, with respect to the web-camera coordinate system denoted by $\{C\}$, of each extracted corner of the physical reference is

three-dimensionally estimated, following (8). Then, the estimated position, with respect to $\{C\}$, of each extracted corner of the physical reference is transformed into with respect to $\{P\}$, following (9). The average position of the extracted corners of the physical reference is considered as the origin position of the coordinate system of the physical reference, denoted by $\{R\}$. Later, the Z-axis of $\{R\}$ is estimated with respect to $\{P\}$, using the linear least-square optimization proposed by T. F. Coleman and Y. Li [48]. Let ${}^P\mathbf{X}_{C1}$, ${}^P\mathbf{X}_{C2}$, ${}^P\mathbf{X}_{C3}$, and ${}^P\mathbf{X}_{C4}$ be the transformed position, with respect to $\{P\}$, of the extracted corners of the physical reference, which are descendingly sorted due to the first component of each extracted corner, ${}^P\mathbf{O}_R$ be the origin of $\{R\}$, with respect to $\{P\}$, and ${}^P\hat{\mathbf{Z}}_R$ be the unit vector of the Z-axis of $\{R\}$, with respect to $\{P\}$. The optimization function of ${}^P\hat{\mathbf{Z}}_R$ can be defined as follows,

$$\mathbf{F}({}^P\hat{\mathbf{Z}}_R) = \begin{bmatrix} ({}^P\mathbf{X}_{C1} - {}^P\mathbf{O}_R)^T \\ ({}^P\mathbf{X}_{C2} - {}^P\mathbf{O}_R)^T \\ ({}^P\mathbf{X}_{C3} - {}^P\mathbf{O}_R)^T \\ ({}^P\mathbf{X}_{C4} - {}^P\mathbf{O}_R)^T \end{bmatrix} {}^P\hat{\mathbf{Z}}_R \quad (11)$$

, while the fourth component of ${}^P\hat{\mathbf{Z}}_R$ empirically equals zero. If ${}^P\mathbf{O}_R$ and ${}^P\hat{\mathbf{Z}}_R$ are resolved, the XY-plane of $\{R\}$ is also determined. After that, ${}^P\mathbf{X}_{C3}$ and ${}^P\mathbf{X}_{C4}$ are rotated about ${}^P\hat{\mathbf{Z}}_R$ through 180° . Next, the rotated points together with ${}^P\mathbf{X}_{C1}$ and ${}^P\mathbf{X}_{C2}$ are categorized into two groups, using the k-means clustering. Later, the points in each group are averaged, and the average point of each group is projected onto the XY-plane of $\{R\}$. Then, two unit vectors with the directions from ${}^P\mathbf{O}_R$ to the projected points, and two unit vectors with the directions from the projected points to ${}^P\mathbf{O}_R$, are defined. Let ${}^P\hat{\mathbf{N}}_1$, ${}^P\hat{\mathbf{N}}_2$, ${}^P\hat{\mathbf{N}}_3$, and ${}^P\hat{\mathbf{N}}_4$ be the defined unit vectors with respect to $\{P\}$, which are descendingly sorted by the first component of each unit vector, ${}^P\hat{\mathbf{X}}_R$ be the unit vector of the X-axis of $\{R\}$, with respect to $\{P\}$, and ${}^P\hat{\mathbf{Y}}_R$ be the unit vector of the Y-axis of $\{R\}$, with respect to $\{P\}$. If the angle between ${}^P\hat{\mathbf{N}}_1$ and ${}^P\hat{\mathbf{N}}_2$ is less than or equal to 90° , ${}^P\hat{\mathbf{X}}_R$ is resolved as follows,

$${}^P\hat{\mathbf{X}}_R = \left\| {}^P\hat{\mathbf{N}}_1 + {}^P\hat{\mathbf{N}}_2 \right\|^{-1} ({}^P\hat{\mathbf{N}}_1 + {}^P\hat{\mathbf{N}}_2). \quad (12)$$

Otherwise, the angle between ${}^P\hat{\mathbf{N}}_1$ and ${}^P\hat{\mathbf{N}}_2$ is greater than 90° , ${}^P\hat{\mathbf{X}}_R$ is determined as follows,

$${}^P\hat{\mathbf{X}}_R = \left\| {}^P\hat{\mathbf{N}}_1 + {}^P\hat{\mathbf{N}}_3 \right\|^{-1} ({}^P\hat{\mathbf{N}}_1 + {}^P\hat{\mathbf{N}}_3). \quad (13)$$

By rotating ${}^P\hat{\mathbf{X}}_R$ about ${}^P\hat{\mathbf{Z}}_R$ through 90° , ${}^P\hat{\mathbf{Y}}_R$ is obtained. Finally, the position, with respect to $\{P\}$, of the physical reference is determined with the homogeneous transformation matrix from $\{R\}$ to $\{P\}$, denoted by ${}^P_R\mathbf{H}$, as follows,

$${}^P_R\mathbf{H} = \begin{bmatrix} {}^P\hat{\mathbf{X}}_R & {}^P\hat{\mathbf{Y}}_R & {}^P\hat{\mathbf{Z}}_R & {}^P\mathbf{O}_R \end{bmatrix}. \quad (14)$$

3.3 System integration

3.3.1 New expression of Gcode motion commands

Normally, any Gcode motion command of the 3D printing expresses the corresponding motion with the target position, with respect to the coordinate system of any 3D printer denoted by $\{P\}$, as demonstrated in Table 2. However, the 3D printing is expected to be performed at any position constrained to any physical reference in this research, while the position of the physical references is initially unrecognized. Hence, any Gcode motion command in this research must originally express the corresponding motion with the target position with respect to the coordinate system of any physical reference, denoted by $\{R\}$, instead of with respect to $\{P\}$. After the homogeneous transformation matrix from $\{R\}$ to $\{P\}$, denoted by ${}^P_R\mathbf{H}$, is estimated using the machine vision, the target position of the Gcode motion command is able to be transformed into with respect to $\{P\}$. Let ${}^R\mathbf{X}$ be the target position, with respect to $\{R\}$ of any Gcode motion command, and ${}^P\mathbf{X}$ be the target position, with respect to $\{P\}$ of the Gcode motion command. Mathematically, ${}^R\mathbf{X}$ is transformed into ${}^P\mathbf{X}$ as follows,

$${}^P\mathbf{X} = {}^P_R\mathbf{H} {}^R\mathbf{X}. \quad (15)$$

If the Gcode command list of any product is modified by transforming ${}^R\mathbf{X}$ into ${}^P\mathbf{X}$ following (15), any applicable 3D printer is capable of fabricating the product at a desirable position constrained to the physical reference, which is specified in the Gcode command list of the product, with the modified Gcode command list of the product. The process flow of fabricating any product at any position constrained to any physical reference using the machine vision integrated 3D printing system is briefly demonstrated in Figure 16.

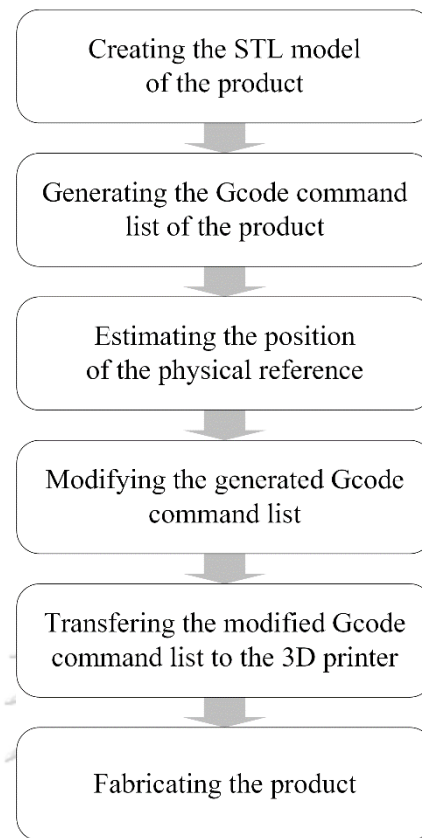


Figure 16 The process flow of fabricating any product at any position constrained to any physical reference using the machine vision integrated 3D printing system.

3.3.2 Hardware

The hardware of the system integration consists of only the computer. On the computer, the Gcode motion command list of any product, generated by the printing-description generating program of the 3D printing, is modified.

3.3.3 Software

The software of the system integration comprises only a system-integration program, which is run on the computer, and was originally developed in this research. The main responsibility of the system integration program is modifying the Gcode command list of any product. So, the target position, with respect to the coordinate system of any physical reference denoted by $\{R\}$, of any Gcode motion command in the Gcode command list of the product is transformed into with respect to the 3D-printer coordinate system, denoted by $\{P\}$ with and the homogeneous transformation matrix from $\{R\}$ to $\{P\}$, denoted by ${}^P_R\mathbf{H}$. Before the system-

integration program is started, the Gcode command list of any product must be generated following the new expression of Gcode motion commands, and ${}^P_R\mathbf{H}$ must be estimated. Firstly, the generated Gcode motion command list of the product and ${}^P_R\mathbf{H}$ are acquired into the system-integration program. Then, the target position, with rest to $\{R\}$, of any Gcode motion command in the generated Gcode command list of the product is transformed into with respect $\{P\}$, following (15). The collaboration of the software of the system integration is shown in Figure 17.

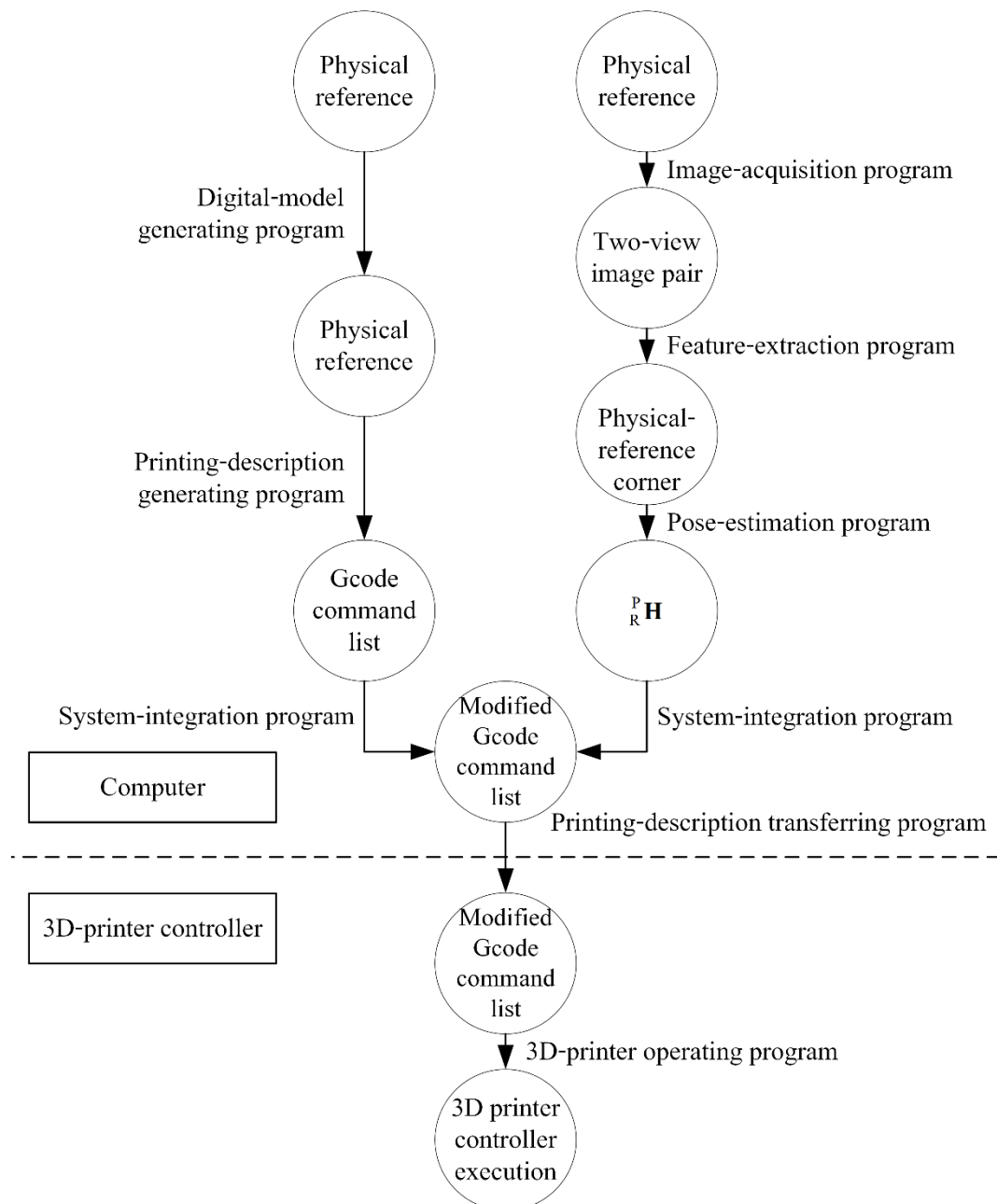


Figure 17 The collaboration of the software of the system integration.

CHAPTER 4

EVALUATION

This chapter mentions the process and result of evaluating the machine vision integrated 3D printing system, on fabricating any product at any position constrained to any physical reference. There are two parts in this chapter. The earlier part involves proving printing capability of the machine vision integrated 3D printing system, while the later part includes determining printing inaccuracy of the machine vision integrated 3D printing system. Moreover, plastic dispenser needles of gauge 18, which have the venting diameter of 0.838 mm, had been equipped to the evaluating plastic syringes evaluation. Additionally, the necessary calibration mentioned in Chapter 3.2.1 was entirely processed, before the evaluation was begun.

4.1 Printing capability

For proving the printing capability of the machine vision integrated 3D printing system, an evaluating product was fabricated, with chocolate frosting, on a rectangular cracker, as an evaluating physical reference, using the machine vision integrated 3D printing system. The process of proving fabrication comprises four steps, including creating the STL model of the evaluating product, generating the Gcode command list of the evaluating product, estimating the position of the evaluating physical reference, and fabricating the evaluating product.

4.1.1 Creating the STL model of the printing-capability evaluating product

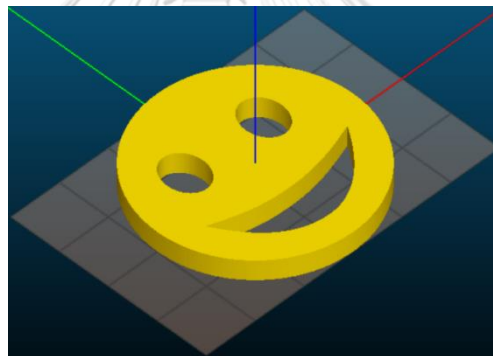
In the digital-model generating program, the evaluating product was manually designed, as a 3D smiley shown in Figure 18, then the STL model of the evaluating product was generated. The thickness and outer diameter of the evaluating product are respective 4 mm and 40 mm.



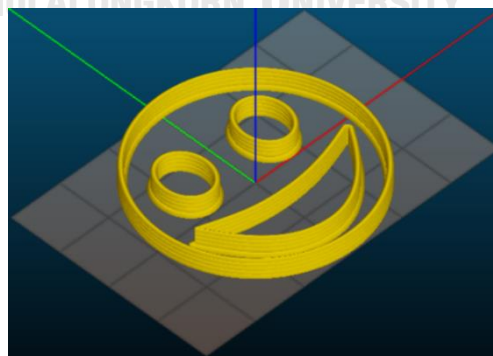
Figure 18 The design of the printing-capability evaluating product.

4.1.2 Generating the Gcode command list of the printing-capability evaluating product

Initially, the printing configuration of the evaluating product was defined in the printing-description generating program, with the extruding factor of 1.2, the layer height of 0.8 mm, the extrusion width of 1 mm, the scanning speed of 5 mm/s, no infill, no horizontal shell, and a single vertical shell. After the STL model of the evaluating product was generated, the STL model was imported into the printing-description generating program. Next, the position, with respect to the coordinate system of the evaluating physical reference, of the evaluating product, was graphically specified, as demonstrated in Figure 19(a). Afterwards, the Gcode command list of the evaluating product was generated, from the printing-description generating program. Following the generated Gcode command list, the evaluating product is supposed to be fabricated as illustrated in Figure 19(b). In addition, the Z-axis of the coordinate system of the evaluating physical reference is denoted by the blue line in Figure 19.



(a) The determined printing position

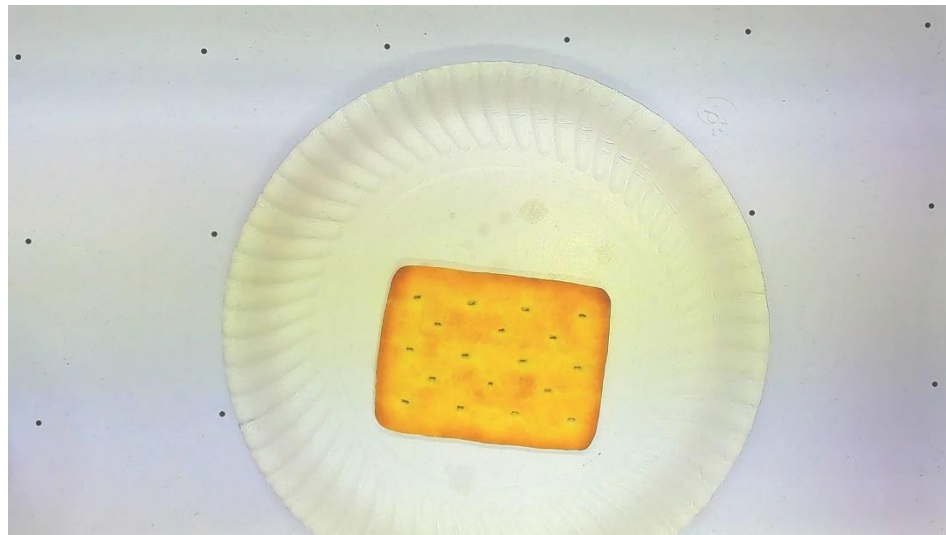


(b) The expectation model

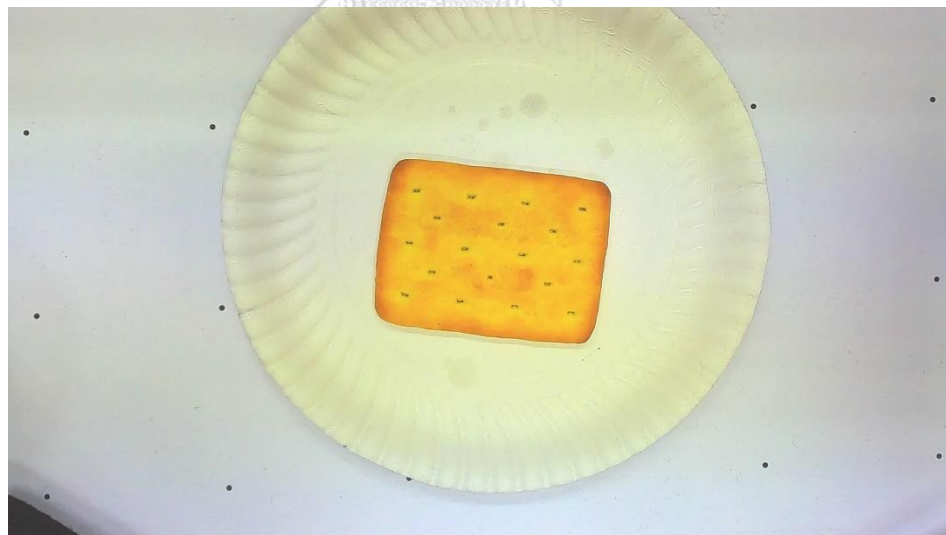
Figure 19 The printing-capability evaluating product in the printing-description generating program.

4.1.3 Estimating the position of the printing-capability evaluating physical reference

Initially, the evaluating physical reference was randomly positioned in the workspace of the 3D printer. Then, the image-acquisition program was processed. A two-view image pair of the evaluating physical reference was successfully acquired into the computer, as shown in Figure 20.



(a) The primary image



(b) The secondary image

Figure 20 The acquired two-view image pair of the printing-capability evaluating physical reference.

After the two-view image pair of the evaluating physical reference was acquired into the computer, the feature-extraction program was processed. For the color thresholding on the

primary image of the two-view image pair, the applied 8-bit RGB threshold has the crossing color value of 0 to 125 for blue, and 0 to 255 for red and green. In order to extract the corners of the evaluating physical reference in the primary image of the two-view image pair from the obtained binary image, the minimum corner quality was specified with the predefined threshold [42] of 0.5. Meanwhile, the Gaussian filtering was done with the filter size [43] of 201 by 201 pixels, and the filter standard deviation [43] of 67. The corners of the evaluating physical reference in the primary image of the two-view image pair were successfully extracted, as demonstrated with the obtained binary image in Figure 21. For tracking the corners of the evaluating physical reference in the secondary image of the two-view image pair, the pyramidal implementation of the KLT algorithm was calculated with the deepest pyramid level [47] of 3, and the integration window size [47] of 101 by 101 pixels. Additionally, the forward-backward error [49] was limited at 0.5 pixels. Meanwhile, the maximum iteration steps [47] was marked at 200 times. The corners of the evaluating physical reference in the secondary image of the two-view image pair were effectively tracked, as illustrated in Figure 22.

After the corners of the evaluating physical reference were completely extracted from the acquired two-view image pair, the pose-estimation program was processed. The position, with respect to the 3D-printer coordinate system, of the evaluating physical reference was completely estimated, as illustrated by the coordinate system in Figure 23.

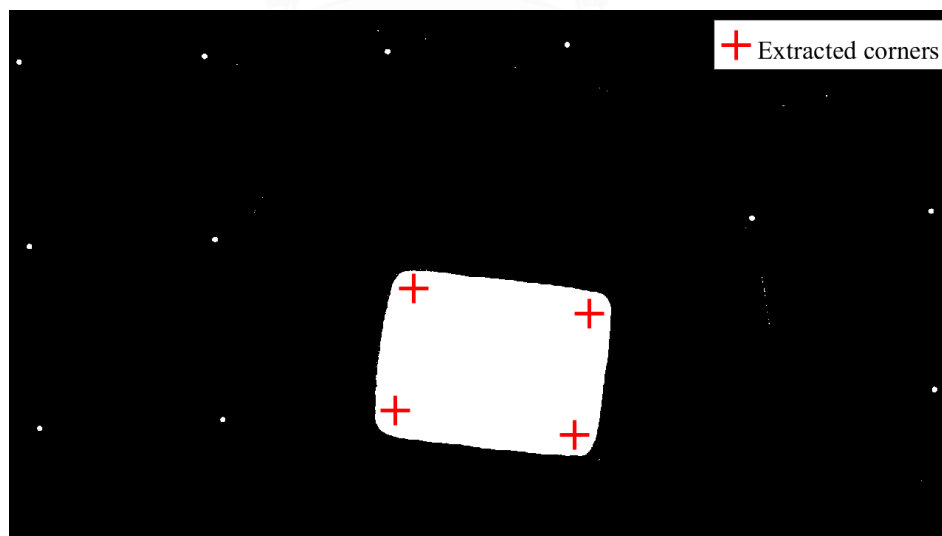


Figure 21 The corners of the printing-capability evaluating physical reference extracted from the primary image of the acquired two-view image pair of the evaluating physical reference.

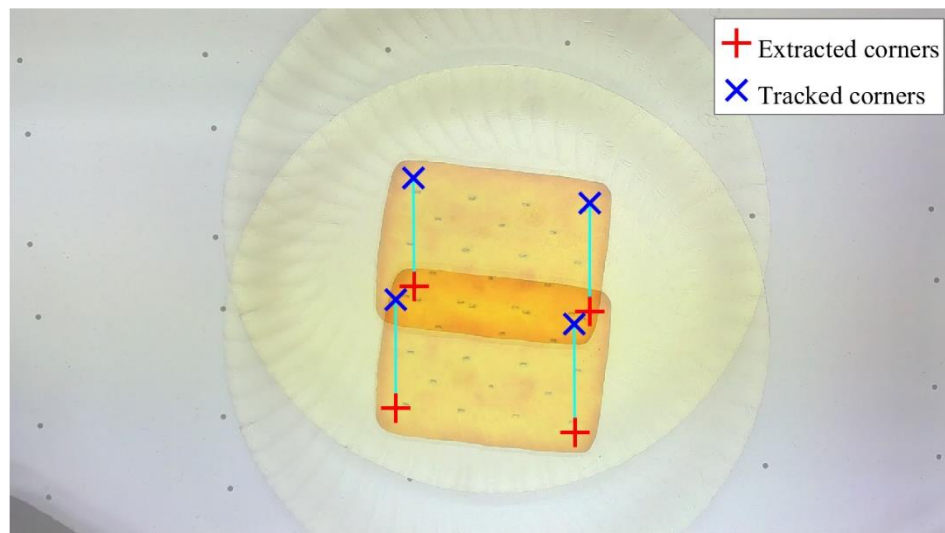


Figure 22 The corners of the printing-capability evaluating physical reference physical reference tracked in the secondary image of the acquired two-view image pair of the evaluating physical reference.

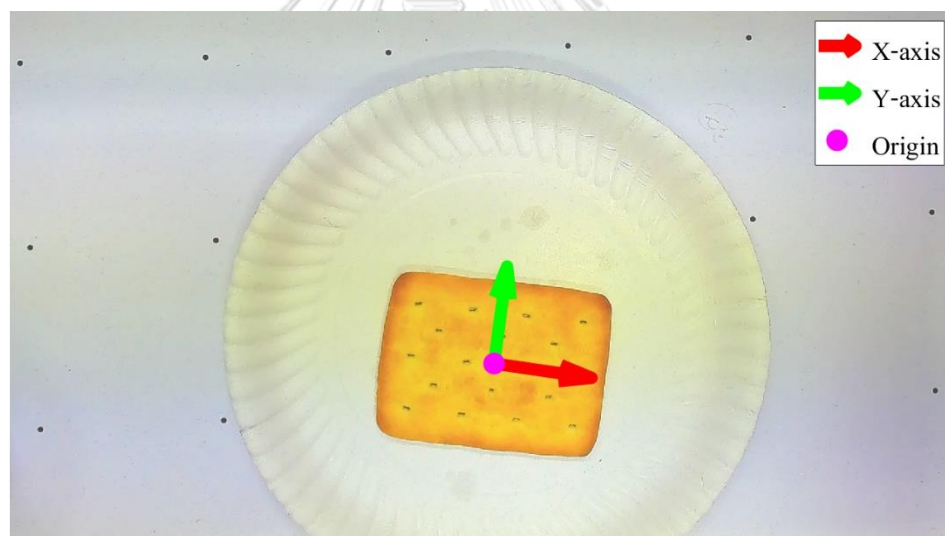


Figure 23 The estimated coordinate system of the printing-capability evaluating physical reference.

4.1.4 Fabricating the printing-capability evaluating product

Initially, the system-integration program was processed. Hence, the generated Gcode command list of the evaluating product was modified. Later, the modified Gcode command list of the evaluating product was transferred into the 3D-printer controller, synchronously with working of the 3D printer, using the printing-description transferring program. Meanwhile, the 3D-printer

operating program was processed, in order to manage execution of the 3D-printer controller following transferred Gcode commands. Thus, the 3D printer accurately fabricated the evaluating product on the evaluating physical reference. Finally, the evaluating product was successfully fabricated on the evaluating physical reference, and the fabricated result of the evaluating product is demonstrated in Figure 24.



(a) The comparable view



(b) The top view

Figure 24 The fabricated result of the printing-capability evaluating product.

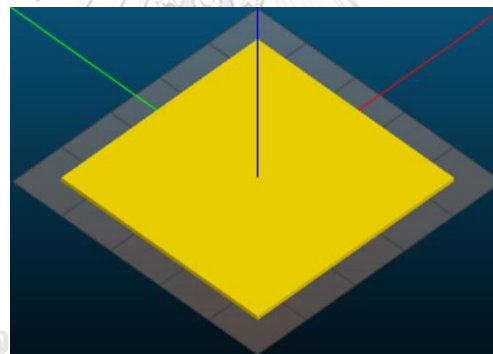
4.2 Printing inaccuracy

In order to determine the printing inaccuracy of the machine vision integrated 3D printing system, evaluating products were fabricated, with silicone sealant, on rectangular acrylic plates, as evaluating physical references, using the machine vision integrated 3D printing system. The process of determining the printing inaccuracy of the machine vision integrated 3D printing system comprises two steps, including fabricating the evaluating products, and estimating the deviated positions of the evaluating products. In addition, the deviated positions of the evaluating

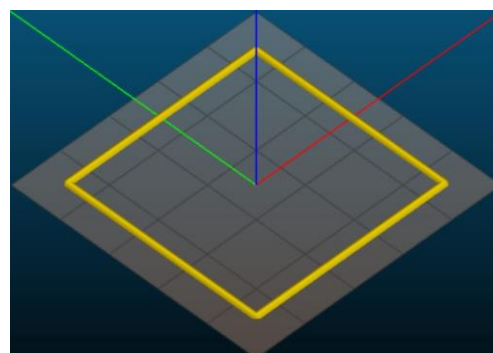
products, which were estimated in this research, are combinedly caused by the system parts of the 3D printing and the machine vision of the machine vision integrated 3D printing system.

4.2.1 Fabricating the printing-inaccuracy evaluating products

Initially, all of the evaluating products were fabricated following the process mentioned in Chapter 4.1. Meanwhile, the evaluating products were redesigned, as thin square plates shown in Figure 25(a). Moreover, the printing configuration of the evaluating products was adjusted, with the extruding factor of 1, the layer height of 0.8 mm, the extrusion width of 1.5 mm, the scanning speed of 5mm/s, no infill, no horizontal shell, and a single vertical shell. Following the generated Gcode command list of the evaluating products, the evaluating products are single-line squares, as illustrated in Figure 25(b). Finally, the evaluating products were successfully fabricated on the evaluating physical references, and the fabricated results of the evaluating products are entirely demonstrated in Figure 26.



(a) The determined printing position



(b) The expectation model

Figure 25 The printing-inaccuracy evaluating products in the printing-description generating program.

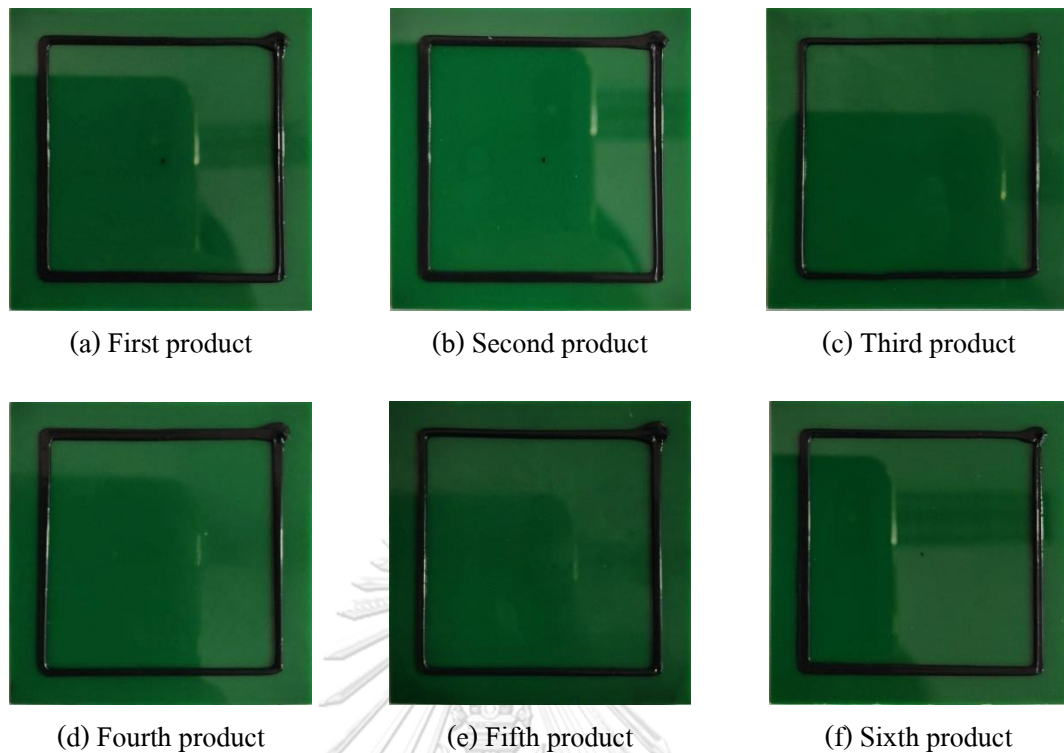


Figure 26 The fabricated results of the printing-inaccuracy evaluating products.

4.2.2 Estimating the deviated positions of the printing-inaccuracy evaluating products

After all of the evaluating products were completely fabricated, the deviated positions of the evaluating products, with respect to the coordinate systems of the evaluating products, were estimated by comparing the position of each evaluating product with the position of the corresponding evaluating physical reference. The process of estimating the position of each evaluating product, and each physical system, is similar to the process mentioned in Chapter 3.2.3, but any position was defined with respect to the web-camera coordinate system instead of the 3D-printer coordinate system. Particularly, the deviated position of each evaluating product is described with a set of Z-Y-X Euler angles, and a translation vector, in this research. Finally, the deviated positions of the evaluating products were successfully estimated, as shown in Table 3. The largest sizes of the individual estimated Z-Y-X Euler angles are respective 0.3236° , 0.9153° , and 2.7450° . Furthermore, the largest sizes of the individual components of the estimated translation vectors, in order of X-axis, Y-axis, and Z-axis, are respective 0.3419 mm, 0.3388 mm, and 0.5769 mm.

Table 3 The deviated positions of the printing-inaccuracy evaluating products.

Product no.	Z-Y-X Euler angles (°)			Translation vector (mm)		
	Z	Y	X	X	Y	Z
1	-0.0822	-0.9083	1.3467	0.0336	0.1908	0.0872
2	-0.2844	-0.8301	-0.2310	0.2999	0.0436	-0.4932
3	-0.2888	-0.2020	0.1812	0.1690	0.1170	-0.4975
4	0.2918	-0.9153	2.7450	0.3419	0.3190	-0.3049
5	0.3236	-0.7831	0.7241	0.1146	0.3388	-0.5769
6	-0.0470	-0.6684	0.4170	0.1924	0.1674	-0.4442

CHAPTER 5

CONCLUSION

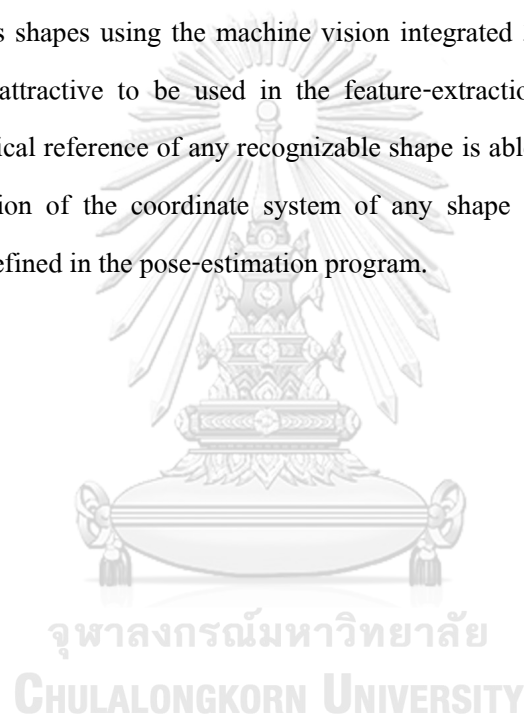
In this chapter, principal points of this research are wrapped up, and recommendation for related future works of this research is presented. Accordingly, these topics are separately expressed in two parts of this chapter.

5.1 Research conclusion

Normally, the 3D printing could not be conveniently and affordably implemented many fabricating applications, in which any product is expected to be fabricated at any position constrained to any physical reference. Hence, this research aimed to resolve this limitation by proposing the machine vision integrated 3D printing system, which physically comprises the designed and constructed 3D printer, the web camera, and the computer. Specifically, any printing description is a Gcode command list in this research. For integrating the machine vision to the 3D printing, the target position of any Gcode motion command is initially defined with respect to the coordinate system of any physical reference. After the position, with respect to the 3D-printer coordinate system, of the physical reference is estimated using the machine vision, the target position of any Gcode motion command is transformed into with respect to the 3D-printer coordinate system. From the successfully fabricated results of the evaluating products, the machine vision integrated 3D printing system is empirically capable of fabricating any product at any desirable position constrained to any physical reference, with fair printing accuracy. In the process flow of fabricating the evaluating products, the position, with respect to the 3D-printer coordinate system, of each evaluating physical reference was conveniently estimated. Moreover, the machine vision integrated 3D printing system costs a budget of the same scale as the 3D printer. Consequently, the machine vision integrated 3D printing system gives promise of conveniently, affordably, and accurately, implementing the 3D printing in many fabricating applications, in which any products is expected to be geometrically customized, and fabricated at the corresponding functional position constrained to a physical reference.

5.2 Recommendation

In this research, some limitations of using the machine vision integrated 3D printing system have not resolved yet. Firstly, the image capturing position of the primary image of any two-view image pair was manually specified in this research. In order to process the image-acquisition program without manually specifying any image capturing position, panoramic image stitching [50] is interesting to be employed in the image-acquisition program. Furthermore, the feature-extraction program and the-pose estimation program were particularly developed for any physical reference of rectangular plate in this research. In order to fabricate products on physical references of various shapes using the machine vision integrated 3D printing system, 3D-shape recognition [51] is attractive to be used in the feature-extraction program. Accordingly, the position of any physical reference of any recognizable shape is able to be automatically estimated, although the definition of the coordinate system of any shape of referencing objects is still necessary to be predefined in the pose-estimation program.



REFERENCES

- [1] K. Ramdas, "Managing product variety: An integrative review and research directions," *Production and Operations Management*, vol. 12, no. 1, pp. 79-101, March 2003.
- [2] X. Du, J. Jiao, and M. Tseng, "Understanding customer satisfaction in product customization," *International Journal of Advanced Manufacturing Technology*, vol. 31, no. 3-4, pp. 396-406, November 2006.
- [3] D. Dimitrov, K. Schreve, and N. de Beer, "Advances in three dimensional printing - State of the art and future perspectives," *Rapid Prototyping Journal*, vol. 12, no. 3, pp. 136-147, 2006.
- [4] B. Berman, "3-D printing: The new industrial revolution," *Business Horizons*, vol. 55, no. 2, pp. 155-162, March 2012.
- [5] K. Subrin, T. Bressac, S. Garnier, A. Ambiehl, E. Paquet, and B. Furet, "Improvement of the mobile robot location dedicated for habitable house construction by 3D printing," *IFAC-PapersOnLine*, vol. 51, no. 11, pp. 716-721, 1 January 2018.
- [6] F. W. Baumann, O. Kopp, and D. Roller, "Abstract API for 3D printing hardware and software resources," *International Journal of Advanced Manufacturing Technology*, vol. 92, no. 1-4, pp. 1519-1535, 1 September 2017.
- [7] J. W. Choi *et al.*, "Development of a mobile fused deposition modeling system with enhanced manufacturing flexibility," *Journal of Materials Processing Technology*, vol. 211, no. 3, pp. 424-432, 1 March 2011.
- [8] N. Bausch, D. P. Dawkins, R. Frei, and S. Klein, "3D printing onto unknown uneven surfaces," *IFAC-PapersOnLine*, vol. 49, no. 21, pp. 583-590, 2016.
- [9] X. Z. Chen and S. B. Chen, "The autonomous detection and guiding of start welding position for arc welding robot," *Industrial Robot*, vol. 37, no. 1, pp. 70-78, 2010.
- [10] N. R. Corby Jr, "Machine Vision for Robotics," *IEEE Transactions on Industrial Electronics*, vol. IE-30, no. 3, pp. 282-291, August 1983.
- [11] K. Chitra, S. Dinesh, D. Mishra, V. Brinda, V. R. Lalithambika, and B. M. Kumar, "3D information retrieval for visual odometry system of planetary exploration rovers - A stereo vision approach," in *International Conference on Advances in Computing, Communications*

- and Informatics*, Mysore, India, 22-25 August 2013, pp. 354-360.
- [12] J. M. Pearce, N. C. Anzalone, and C. L. Heldt, "Open-source wax RepRap 3-D printer for rapid prototyping paper-based microfluidics," *Journal of Laboratory Automation*, vol. 21, no. 4, pp. 510-516, 1 August 2016.
- [13] M. Lau, J. Mitani, and T. Igarashi, "Digital fabrication," *Computer*, vol. 45, no. 12, pp. 76-79, 2012.
- [14] M. P. Groover, *Fundamentals of modern manufacturing : materials, processes, and system*, 3rd ed. Hoboken, N.J: John Wiley, 2007.
- [15] S. H. Huang, P. Liu, A. Mokasdar, and L. Hou, "Additive manufacturing and its societal impact: A literature review," *International Journal of Advanced Manufacturing Technology*, Review vol. 67, no. 5-8, pp. 1191-1203, July 2013.
- [16] S. Lim, R. A. Buswell, T. T. Le, S. A. Austin, A. G. F. Gibb, and T. Thorpe, "Developments in construction-scale additive manufacturing processes," *Automation in Construction*, vol. 21, no. 1, pp. 262-268, January 2012.
- [17] G. Wang, L. Yao, W. Wang, J. Ou, C. Y. Cheng, and H. Ishii, "XPrint: A modularized liquid printer for smart materials deposition," in *Conference on Human Factors in Computing Systems*, San Jose, CA, 7 May 2016, pp. 5743-5752.
- [18] M. Peña-Cabrera, I. Lopez-Juarez, R. Rios-Cabrera, and J. Corona-Castuera, "Machine vision approach for robotic assembly," *Assembly Automation*, vol. 25, no. 3, pp. 204-216, 2005.
- [19] Z. Sun, G. Bebis, and R. Miller, "On-road vehicle detection: A review," *IEEE Transactions on Pattern Analysis and Machine Intelligence*, vol. 28, no. 5, pp. 694-711, May 2006.
- [20] P. Turaga, R. Chellappa, V. S. Subrahmanian, and O. Udrea, "Machine recognition of human activities: A survey," *IEEE Transactions on Circuits and Systems for Video Technology*, vol. 18, no. 11, pp. 1473-1488, November 2008.
- [21] H. Golnabi and A. Asadpour, "Design and application of industrial machine vision systems," *Robotics and Computer-Integrated Manufacturing*, vol. 23, no. 6, pp. 630-637, December 2007.
- [22] F. Kurtulmus, W. S. Lee, and A. Vardar, "Green citrus detection using 'eigenfruit', color and circular Gabor texture features under natural outdoor conditions," *Computers and*

- Electronics in Agriculture*, vol. 78, no. 2, pp. 140-149, September 2011.
- [23] C. Pappone *et al.*, "Robotic magnetic navigation for atrial fibrillation ablation," *Journal of the American College of Cardiology*, vol. 47, no. 7, pp. 1390-1400, 7 April 2006, doi: 10.1016/j.jacc.2005.11.058.
- [24] P. Abolmaesumi, S. E. Salcudean, W. H. Zhu, M. R. Sirouspour, and S. P. DiMaio, "Image-guided control of a robot for medical ultrasound," *IEEE Transactions on Robotics and Automation*, Article vol. 18, no. 1, pp. 11-23, February 2002.
- [25] R. Y. Tsai, "A versatile camera calibration technique for high-accuracy 3D machine vision metrology using off-the-shelf TV cameras and lenses," *IEEE Journal on Robotics and Automation*, August vol. 3, no. 4, pp. 323-344, 1987.
- [26] J. Heikkila and O. Silven, "A four-step camera calibration procedure with implicit image correction," in *Proceedings of the IEEE Computer Society Conference on Computer Vision and Pattern Recognition*, 1997, pp. 1106-1112.
- [27] R. Hartley and A. Zisserman, *Multiple View Geometry in Computer Vision*, 2nd ed. Cambridge, United Kingdom: Cambridge University Press, 2004.
- [28] K. Konolige, "Small Vision Systems: Hardware and Implementation," in *The International Symposium of Robotics Research*, Hayama, Japan, 3-7 October 1997, pp. 203-212.
- [29] D. J. Horrobin and R. M. Nedderman, "Die entry pressure drops in paste extrusion," *Chemical Engineering Science*, Article vol. 53, no. 18, pp. 3215-3225, 1998.
- [30] B. Wijnen, E. J. Hunt, G. C. Anzalone, and J. M. Pearce, "Open-source syringe pump library," *PLoS ONE*, vol. 9, no. 9, 2014.
- [31] D. G. Alciatore and M. B. Hestand, *Introduction to mechatronics and measurement systems*, 4th ed. New York, NY: McGraw-Hill, 2011.
- [32] J. S. Chen, Y. K. Huang, and C. C. Cheng, "Mechanical model and contouring analysis of high-speed ball-screw drive systems with compliance effect," *International Journal of Advanced Manufacturing Technology*, Article vol. 24, no. 3-4, pp. 241-250, 2004.
- [33] J. J. Craig, *Introduction to robotics : mechanics and control*, 3rd ed. Upper Saddle River, N.J: Pearson Prentice Hall, 2005.
- [34] M. Szilvási-Nagy and G. Mátyási, "Analysis of STL Files," *Mathematical and Computer Modelling*, Conference Paper vol. 38, no. 7-9, pp. 945-960, 2003.

- [35] F. W. Baumann, M. Schuermann, U. Odefey, and M. Pfeil, "From GCode to STL: Reconstruct Models from 3D Printing as a Service," in *International Conference on Mechanical Engineering and Automation Science*, Birmingham, UK, 13-15 October 2017, vol. 280.
- [36] Z. Zhang, "A flexible new technique for camera calibration," *IEEE Transactions on Pattern Analysis and Machine Intelligence*, vol. 22, no. 11, pp. 1330-1334, 2000.
- [37] T. F. Coleman and Y. Li, "On the convergence of interior-reflective Newton methods for nonlinear minimization subject to bounds," *Mathematical Programming*, vol. 67, no. 2, pp. 189-224, November 1994.
- [38] T. F. Coleman and Y. Li, "An interior trust region approach for nonlinear minimization subject to bounds," *SIAM Journal on Optimization*, vol. 6, no. 2, pp. 418-445, May 1996.
- [39] M. C. Yang, K. L. Liu, and S. Y. Chien, "A real-time FHD learning-based super-resolution system without a frame buffer," *IEEE Transactions on Circuits and Systems II: Express Briefs*, vol. 64, no. 12, pp. 1407-1411, 2017.
- [40] R. A. A. Raof *et al.*, "Color thresholding method for image segmentation algorithm of Ziehl-Neelsen sputum slide images," in *International Conference on Electrical Engineering, Computing Science and Automatic Control*, Mexico City, Mexico, 12-14 November 2008, pp. 212-217.
- [41] N. B. A. Mustafa *et al.*, "Image processing of an agriculture produce: Determination of size and ripeness of a banana," in *International Symposium on Information Technology*, Kuala Lumpur, Malaysia, 26-29 August 2008, vol. 1.
- [42] J. Shi and C. Tomasi, "Good features to track," in *Proceedings of the IEEE Computer Society Conference on Computer Vision and Pattern Recognition*, Seattle, WA, 21-23 June 1994, pp. 593-600.
- [43] K. Zhang, L. Zhang, H. Song, and W. Zhou, "Active contours with selective local or global segmentation: A new formulation and level set method," *Image and Vision Computing*, vol. 28, no. 4, pp. 668-676, 2010.
- [44] D. Arthur and S. Vassilvitskii, "K-means++: The advantages of careful seeding," in *Annual ACM-SIAM Symposium on Discrete Algorithms*, New Orleans, LA, 7-9 January 2007, pp. 1027-1035.

- [45] B. D. Lucas and T. Kanade, "An iterative image registration technique with an application to stereo vision," in *International Joint Conference of Artificial Intelligence*, Vancouver, Canada, 1981, vol. 2, pp. 674-679.
- [46] C. Tomasi and T. Kanade, "Detection and tracking of point features," Carnegie Mellon University, April 1991.
- [47] J.-Y. Bouguet, "Pyramidal implementation of the affine lucas kanade feature tracker description of the algorithm," *Intel Corporation*, vol. 5, no. 1-10, p. 4, 2001.
- [48] T. F. Coleman and Y. Li, "A reflective Newton method for minimizing a quadratic function subject to bounds on some of the variables," *SIAM Journal on Optimization*, vol. 6, no. 4, pp. 1040-1058, November 1996.
- [49] Z. Kalal, K. Mikolajczyk, and J. Matas, "Forward-backward error: Automatic detection of tracking failures," in *International Conference on Pattern Recognition*, Istanbul, Turkey, 23-26 August 2010, pp. 2756-2759.
- [50] M. Brown and D. G. Lowe, "Automatic panoramic image stitching using invariant features," *International Journal of Computer Vision*, vol. 74, no. 1, pp. 59-73, 1 August 2007.
- [51] H. Su, S. Maji, E. Kalogerakis, and E. Learned-Miller, "Multi-view convolutional neural networks for 3D shape recognition," in *IEEE International Conference on Computer Vision*, Santiago, Chile, 11-18 December 2015, pp. 945-953.

VITA

NAME Chaiwuth Sithiwichankit
DATE OF BIRTH 21 May 1995
PLACE OF BIRTH Bangkok, Thailand
INSTITUTIONS ATTENDED B.Eng., Chulalongkorn University
HOME ADDRESS Bangkok, Thailand

